Root-associated microbiomes of Gymnadenia conopsea under the combined effect of plant geographical location and developmental stage

Zhinan Mei (meizhinan@163.com)
South-Central University for Nationalities https://orcid.org/0000-0002-2354-8787
Min Lin
South Central University for Nationalities
Hui Xiong
South Central University for Nationalities
Xuechuan Xiang
South Central University for Nationalities
Zelin Zhou
South Central University for Nationalities
lifeng Liang
South Central University for Nationalities

Research

Keywords: Gymnadenia conopsea, root-associated microbiomes, geographical location, developmental stage

Posted Date: January 22nd, 2020

DOI: https://doi.org/10.21203/rs.2.21631/v1

Root-associated microbiomes of *Gymnadenia conopsea* under the combined effect of plant geographical location and developmental stage

Min Lin[1 †], Hui Xiong[1†], Xuechuan Xiang[1], ZelinZhou[1], lifeng Liang[2*] and Zhinan Mei[1*]

1 School of Pharmaceutical Sciences, South-Central University for Nationalities, Wuhan, China

2 Institute of Ethnomedicine, South-Central University for Nationalities, Wuhan, China

† Min Lin and Hui Xiong contributed equally to this work.

* Correspondence: llfgz1991@outlook.com; meizhinan@163.com

Abstract

Background: *Gymnadenia conopsea* (L.) R. Br. is an important perennial terrestrial photosynthetic orchid species whose microbiomes are thought to play an important role in promoting its growth and health. However, the assemblage of *G. conopsea* root-associated microbial communities is poorly understood.

Results: The compositions of fungal and bacterial communities from the roots and corresponding soil samples of *G. conopsea* across distinct biogeographical regions from two significantly different altitudes were characterized at the vegetative and reproductive growth stages. The geographical location, developmental stage and compartment were factors contributing to microbiome variation in *G. conopsea*. Predominant fungal taxa include *Ascomycota*, *Basidiomycota*, *Mortierellomycota* and *Chytridiomycota*, whereas *Proteobacteria*, *Bacteroidetes*, *Acidobacteria*,

Actinobacteria, *Verrucomicrobia*, *Chloroflexi*, *TM7* and *Planctomycetes* were predominant bacterial taxa. The fungi classes of *Leotiomycetes*, *Agaricomycetes*, *Eurotiomycetes* and *Mortierellomycetes*, as well as bacterial taxa *Actinobacteria* were more abundant in *G. conopsea* from higher altitude location. Moreover, Dark septate endophytes and Arbuscular mycorrhiza may have important role for *G. conopsea* to adapt to high altitude environment.

Conclusions: Using *G. conopsea* as a model, we report a comprehensive analysis of the structural and functional composition of the *G. conopsea* root-associated microbiomes. Contrary to previous studies, biogeography was the main factor influencing the microbial community in this study. Although the microbial composition varied greatly by location, the symbiotic microorganisms of *G. conopsea* still have certain specificity. This study offers a robust knowledge of *G. conopsea* root-associated microbiomes and lends guidelines to the investigation of adaptation mechanism of *G. conopsea* in high altitude environment. Our results also laying a foundation for harnessing the microbiome for sustainable *G. conopsea* production. Moreover, these results might be generally applicable to other Orchidaceae plants.

Background

Terrestrial plants harbor abundant and diverse microorganisms that affect plant distribution, growth, and health in a beneficial, harmful, or neutral way. Previous research revealed that plants can recruit beneficial/specific communities to cope with pathogen encounters, modify the nutrient status as well as adapt to new or changing

environmental conditions[1-3]. In addition, the spatial distribution of soil organisms, such as soilborne mutualists, probably acts as a driver of spatial patterns of species within plant communities and plant community diversity[4]. These communities can be regarded as the plant host's extended genome, providing a wide range of potential functional capacities[3, 5]. To enhance plant growth and health, it is essential to investigate the community structure of microorganisms within the plant and their function. So far, most research work has made on certain model and crop plant species, such as *Arabidopsis*[6, 7], rice[8], maize[9], millet[10], *populus*[11], and citrus[12], the results revealed clear taxonomically structured microbiome and the factors that determine assembly of the microbiome. This work may enable new plant management approaches and provide novel tools to improve the robustness of crop plant performance. We hypothesize here that growth and distribution of traditional herbal medicine could be impacted by changes in the microbial community. However, the relative research in traditional herbal medicine is still rare.

Gymnadenia conopsea (L.) R. Br. (Orchidaceae), a terrestrial photosynthetic orchid species geographically widely distributed in Eurasia, including England, Ireland, Russia, Nepal, China, Japan, and the Korean peninsula[13] (Commission of Flora Reipublicae Popularis Sinicae; http://www.eflora.org). *G. conopsea* was found in a wide range of various habitat types that distributed from 200 m to 4700 m altitude in China. For many years, *G. conopsea* was the primary component in many preparations as listed in the Chinese Pharmacopeia, and used as a reinforcing agent of traditional

medicines to improve the body and treat various diseases in China, especially in Tibetan medicine and Mongolian medicine. Whereas *G. conopsea* has been investigated as an important fragrant orchid plant in some European countries. Like most other orchids, this species is declining. Now, *G. conopsea* was list in Convention on International Trade in Endangered Species of Wild Fauna and Flora (CITES). There two aspects have resulted in the rapid decrease of the resources of this plant. The external factors were due to the high market demand, over exploitation combined with the habitat destruction, the internal endangered factors were its weak fertility and low breeding efficiency.

It was known that orchidaceae seeds are remarkably small, extremely light, lacking endosperm (food reserves), the germination rate is very low under natural conditions, and seeds germination in the wild may need colonization by a compatible fungus providing carbohydrates, in addition, fungi are also an indispensable part of the life cycle of Orchidaceae, such as establishment and growth of seedlings (subsequent growth to a seedling)[14]. Early studies on the specificity between Orchidacea plants and their mycorrhizal fungi were mainly based on cultivation methods or germination tests under laboratory conditions and found a considerable phylogenetic breadth of associated fungi[15]. Though it is widely recognized that fungi perform crucial roles in Orchidacea plants plant, the impact of underground root-associated fungi on plant growth and plant biodiversity is less well understood. Meanwhile, fungi cultivation under laboratory conditions does not reflect the complexity of interactions under natural conditions[16, 17]. Furthermore, due to their hidden lifestyle, the fact that many fungi cannot be cultivated under normal laboratory conditions, and it is difficult to manipulate

the presence and diversity of fungi without contamination, or outgrowing contaminants could have additionally biased these early results.

Amplicon based community profiling approaches that amplify a broad taxonomic spectrum of fungi largely eliminate these biases and allow the direct assessment of the fungal diversity present within an orchid root [18-21]. Recent investigations applying molecular methods have shown a more complex picture, pointing to a considerable specificity between some orchid species and their mycorrhizal fungi. Besides, previously study showed that bacteria isolated from orchid also benefit for plant growth and resistance to pathogens[22]. Nevertheless, at present, little is known about the actual distribution of fungi in natural *G.conopsea* populations and how it affects spatial and temporal patterns of recruitment and establishment of *G.conopsea*. Meanwhile, the composition and functional activity of the *G.conopsea*-associated bacteria remains largely unexplored.

For the present study, we collected root and soil samples of the wild-grown *G. conopsea* plants from two different growth locations (habitats) and two developmental stages. The dynamics of fungal and bacterial communities in *G. conopsea* of two distinct compartments from two distinct growth locations at two developmental stages were monitored using ITS2 and 16S rRNA gene amplicon sequencing technology. Multiple factors contributing to microbial community variation were evaluated, and fungal and bacterial functions were predicted according to their taxonomy. The large datasets from

111 the different conditions sampled in this study were used for identification of putative
112 microbial consortia involved in processes such as plateau adaptability. Through
113 dynamic studies of the microbiome composition, we provide insights into the process
114 of *G. conopsea* plants microbiome assembly, laying a foundation for harnessing the
115 microbiome for sustainable *G. conopsea* production.

116

117 **Results**

118 **Root-associated microbial assemblages**

119 We collected *G. conopsea* root and the associated bulk soil samples from two sites with
120 the altitude at 3600 meters (Linzhi, LZ for short) and 496 meters (Greater Khingan
121 Mountains, DXAL for short) separately in China. Linzhi has a plateau temperate semi-
122 humid and humid monsoon climate, whereas Greater Khingan Mountains
123 belongs to the cold-temperate humid continental climate zone. We analyzed fungal and
124 bacterial microbiomes from two separate rhizocompartments (the root and
125 corresponding soil), a total of 145 samples that 69 samples from LZ and 76 samples
126 from DXAL (Additional file 1: Table S1). For this study, soil compartment microbiome
127 was from the surrounding soil of plant; the root compartment microbiome, composed
128 of the microbes inhabiting the interior of the root (Methods). The V3-V4 region of 16S
129 rRNA gene and internal transcribed spacer 2 (ITS2) region of ITS were amplified by
130 PCR and sequenced using Illumina MiSeq platform. Approximately 12.1 and 5.1
131 million high-quality sequence tags were generated for the ITS2 and 16S rRNA gene
132 sequencing samples, respectively. 6,667,165 and 5,460,693 ITS2 tags and 3,883,175

and 1,206,448 16S rRNA tags were generated for each bulk soil and root sample, respectively (Additional file 1: Table S2, 3). After discarding non-bacterial or non-fungi, mitochondrial, chloroplast and low-abundance operational taxonomic units (OTUs), we obtained 9,712 bacterial OTUs and 5,193 fungi OTUs, respectively (Additional file 1: Table S2, 3). For the microbial richness Chao index estimated based on the fungal dataset, it revealed a decrease of microbial richness from soil to the root in both sites (Fig. 1a, $p < 0.05$, Kruskal Wallis with Dunn's post hoc test), except the soil sample in Greater Khingan Mountains at reproductive growth stage. Significant differences were also detected in comparisons between two different developmental stages in root samples include LZ and DXAL, the richness value was higher in the vegetative growth stage than reproductive growth stage. Similar results were retrieved from microbial diversity shannon index estimates, with higher diversity values detected in soil samples (Fig. 1b, $p < 0.05$, Kruskal Wallis with Dunn's post hoc test). For the bacterial microbiomes, measures of within-sample diversity (α-diversity indices) revealed a decrease of microbial richness and diversity from soil to the root based on the chao index and shannon index in both sites (Fig. 1c, d, $p < 0.05$, Kruskal Wallis with Dunn's post hoc test). In both bacterial microbial richness and diversity, higher richness and diversity were observed in vegetative growth stage than reproductive growth stage at two sides ($p < 0.05$, Kruskal Wallis with Dunn's post hoc test).

To examine between-sample variation (β-diversity) and to investigate patterns of separation between microbial communities, principal coordinate analyses (PCoAs)

based on weighted UniFrac (WUF), unweighted UniFrac (UUF) and Bray-Curtis distances were performed. In both the WUF and UUF PCoAs, fungal and bacterial communities cluster along the first principal-coordinate analysis (PCoA) axis according to the geographical location and development stage, the second factor explaining fungal and bacterial communities was slightly different (Fig. 2a WUF, 2b UUF; 2c WUF, 2d, UUF, Additional file 2: Figure S1a, 1b, Bray-Curtis). In fungal community, compartment was the second factor using WUF metric, while not obvious by UUF metric and Bray-Curtis metric (Fig. 2b, Additional file 2: Figure S1a); however, in bacterial community, compartment was the second factor in all metric (Fig. 2c, 2d, Additional file 2: Figure S1b). Interestingly, the PCoA result of the bacterial communities, some samples (include root and soil samples) in the DXAL at reproductive growth stage were close to LZ samples. Additionally, the data for clustering of samples were calculated by permutational multivariate analysis of variance (PERMANOVA) with all distance, which revealed that site, compartment and developmental stage comprise the largest source of variation within the microbiome data in both fungal and bacterial communities, it was consist with the PCoA results [R2 of 0.709 and 0.644 (WUF); 0.462 and 0.429 (UUF); 0.617 and 0.569 (Bray-Curtis) respectively, P value < 0.001 for all tests; Additional file 1: Table S4]. Whereas according to the single factor, site was the strongest factor shaping these microbiome communities, followed by compartment or plant development stage [R2 of 0.272, 0.204, and 0.091 (WUF); 0.203, 0.063, and 0.072 (UUF); 0.303, 0.076, and 0.093 (Bray-Curtis) in fungal community; R2 of 0.244, 0.226, and 0.078 (WUF); 0.177, 0.089, and 0.059

(UUF); 0.223, 0.150, and 0.077 (Bray-Curtis) in bacterial community, for site, compartment, and stage, respectively, P value < 0.001 for all tests; Additional file 1: Table S4]. Together, these results implying that microbial communities vary significantly between plant host biogeography, compartments and developmental stages also impact *G. conopsea* microbial community composition.

Taxonomic assignment of microbial community composition

A totally of 17/39 different phyla and 65/122 different classes were identified in fungal/bacterial communities, respectively. As expected, there were obvious differences in the proportions of various phyla and classes across the compartments that are consistent across each site and development stage (Fig. 3, Additional file 2: Figure S2). The dominant (RA >1%) fungal phyla found in the samples included *Ascomycota* (>50%), *Basidiomycota*, *Mortierellomycota* and *Chytridiomycota*, whereas prokaryotic phyla, included *Proteobacteria* (>28%), *Bacteroidetes*, *Acidobacteria*, *Actinobacteria*, *Verrucomicrobia*, *Chloroflexi*, *TM7* and *Planctomycetes* (Additional file 1: Table S5). At lower taxonomic ranks, *Leotiomycetes*, *Agaricomycetes*, *Dothideomycetes*, *Sordariomycetes*, *Eurotiomycetes*, *Tremellomycetes* and *Mortierellomycetes* were the dominant fungal classes found in both compartments across two sites, *Alphaproteobacteria*, *Betaproteobacteria*, *Deltaproteobacteria*, *Saprospirae*, *Gammaproteobacteria*, *Sphingobacteriia*, *Actinobacteria*, *Acidobacteria-6*, *Thermoleophilia*, *TM7-1*, *Acidimicrobiia*, *Solibacteres*, *Cytophagia* and *Spartobacteria* were the main bacterial classes (Additional file 1: Table S6). The root had a

significantly greater proportion of *Leotiomycetes* and *Tremellomycetes* (q value < 0.05) than soil, whereas *Agaricomycetes*, *Glomeromycetes*, *Lobulomycetes*, *Rhizophydiomycetes* and *Spizellomycetes* (q value < 0.05) are mostly depleted in the root compared with the soil in fungal communities (Wilcoxon test; Additional file 1: Table S7). In the bacterial communities, *Alphaproteobacteria*, Methylacidiphilae, *Sphingobacteriia* and *TM7_3* (q value < 0.01) were more abundant in root, while *Acidobacteria_6*, *AT_s54*, *EC1113*, *Gemm_1*, *Gemm_2*, *Gemm_5*, *Gemmatimonadetes*, *iii1_8*, *ML635J_21*, *Nitrospira*, *OM190*, *Phycisphaerae*, *PRR_12*, *RB25*, *S035*, *S085*, *SJA_28*, *SM2F11*, *TA18*, *TK10*, *TK17* and *TM1* (q value < 0.01) was more prevalent in soil (Wilcoxon test; Additional file 1: Table S8). The reduction in relative abundance of these classes across the compartments is consistent with the observation that microbial diversity decreases from the soil to the root.

Core functional prediction of the microbiome

As microbes that are consistently present across samples likely provide critical ecological functions[23], the core fungal/bacterial communities were analyzed in each group. To examine the core taxonomic structure of the fungal/bacterial communities in each group, we searched for a core microbiome in each group, defined here using a stringent criterion: the set of operational taxonomic units (OTUs) present in more than 90% of the samples. We defined 390/718 core root fungal OTUs and 1190/1314 core soil fungal OTUs from LZ and DXAL microbiota throughout the two growth stages, respectively. Regarding fungal functional group (guild), all core OTU were classify based on FunGuild assignment. Since the whole genome information of fungi is still

relatively scarce, the functional annotation information of fungi is less comprehensive. There were only 38.24% (910/2380) core OTU have reliable functional annotation information. From the trophic mode level, saprotroph was most dominant trophic mode, followed by symbiotroph and pathotroph (Fig. 4a, Additional file 1: Table S9). Undefined_Saprotroph, Plant_Pathogen, Endophyte, Ectomycorrhizal and Animal_Pathogen-Undefined_Saprotroph were the top five high-abundance guilds (Fig. 4b, Additional file 1: Table S9). Such findings were consistent with the fact that *G. conopsea* prefer to humus soil and usually grow associated with mycorrhizas. The Growth_Morphology mainly focus on Microfungus, Agaricoid, Facultative_Yeast, Clavarioid, Yeast, Facultative_Yeast-Microfungus, Dark_Septate_Endophyte, Corticioid, Gasteroid, Thallus and Pezizoid (Fig. 4c, Additional file 1: Table S9).

For the bacterial core OTUs, 1,417/3,099 core root OTUs and 4,403/5,920 core soil OTUs from LZ and DXAL microbiota were obtained throughout the two growth stages, respectively, using the aforementioned method. To increase the insight into functional changes within the *G. conopsea* bacterial microbiome, we determined to what extent different KEGG pathways and modules were enriched in root microbiota compared to soil (Fig. 5, Additional file 1: Table S10). The samples from root displayed higher potential for plant nutrition, such as transport of simple sugars and amino acids, stress resistance, Nodulation (Aromatics degradation, Drug efflux transporter/pump, Drug resistance, Mineral and organic ion transport system, Pathogenicity, Peptide and nickel transport system, Phosphate and amino acid transport system, Plant pathogenicity,

Saccharide, polyol, and lipid transport system and Symbiosis, whereas the modules for Energy metabolism, Nucleotide and amino acid metabolism and Genetic information processing (Aminoacyl tRNA, Aromatic amino acid metabolism, ATP synthesis, Carbon fixation, Cofactor and vitamin biosynthesis, Methane metabolism, Nucleotide sugar, Proteasome, Ribosome and RNA polymerase) were enriched in soil samples (Fig. 5, Additional file 1: Table S10). Nutrition is an important factor that shapes the root microbiome, the root is replete with plant-derived compounds that would be likely nutrient sources for microbes. Consistent with this, the modules that include transport system responsible for transporting phosphate, amino acid, peptide, nickel, Saccharide, polyol, and lipid were over-represented in the core root microbiome. Symbiosis is known to play a role in plant growth due to its function in plant biodiversity and nutrient supply[24], and was observed significantly enriched in root samples compared with soil (Fig. 5). The soil microbiome exhibited increased potential for Carbon fixation, consistent with the enrichment of *Cyanobacteria* in soil samples (Additional file 1: Table S5).

Comparative analyses of core microbiome across different sites

To investigate how plant geographical locations and microhabitat variation might affect the microbiome, the core OTU that significantly different in abundance in each group were used for further analysis, and the community compositions from two plants growth locations were compared (Wilcoxon signed rank test, Benjamini-Hochberg adjusted $P < 0.05$), the difference of fungal community compositions in the root and soil samples under different growth stages from two plants growth locations are shown in Fig. 6 and

Additional file 1: Table S11. Among the root samples, the fungal community composition was notably different between two sites at the vegetative growth stage, *Leotiomycetes*, *Agaricomycetes*, *Eurotiomycetes* and *Mortierellomycetes* were more abundant in LZ core fungal OTUs, whereas *Sordariomycetes*, *Dothideomycetes* and *Tremellomycetes* were more prevalent in DXAL core fungal OTUs (Fig. 6a; Wilcoxon signed rank test, Benjamini-Hochberg adjusted $P < 0.05$); in the soil samples, the relative abundance of *Agaricomycetes*, *Leotiomycetes*, *Eurotiomycetes*, *Mortierellomycetes*, *Orbiliomycetes* and *Rhizophydiomycetes* dramatically higher in LZ compare with DXAL, whereas that of *Sordariomycetes*, *Dothideomycetes*, *Tremellomycetes* and *Pezizomycetes* decreased in LZ (Fig. 6b). The fungal community compositions among samples at the reproductive growth stage were more similar in two sites. In the root samples, *Mortierellomycetes* was more abundant in LZ, whereas *Dothideomycetes* and *Eurotiomycetes* were more prevalent in DXAL (Fig. 6c), as for the soil samples, the relative abundance of *Sordariomycetes*, *Dothideomycetes* and *Eurotiomycetes* were higher in DXAL, whereas that of *Agaricomycetes* was lower in DXAL (Fig. 6d).

The difference of taxonomic structure in the bacterial communities was also examined (Fig. 7, Additional file 2: Figure S3 and Additional file 1: Table S12). *Proteobacteria*, *Bacteroidetes*, *Acidobacteria*, *Actinobacteria*, *Verrucomicrobia*, *Chloroflexi*, *TM7*, *Firmicutes* and *Planctomycetes* as dominating phyla in root bacterial communities at the vegetative growth stage, the relative abundance of these phyla was significantly different between two sites (Fig. 7a). The families belonging to the three dominant

(*Proteobacteria*, *Bacteroidetes* and *Acidobacteria*) phyla were listed, which contained 15 families and belonged to 8 classes (Fig. 7b). *Rhodospirillaceae*, *Hyphomicrobiaceae* and *Rhizobiaceae* (*Alphaproteobacteria*), *Sinobacteraceae* (*Gammaproteobacteria*), *Sphingomonadaceae* (*Bacteroidetes*) are significantly enriched in LZ compared to DXAL at the vegetative growth stage, whereas *Comamonadaceae* and *Oxalobacteraceae* (*Betaproteobacteria*), *Xanthomonadaceae* (*Gammaproteobacteria*), *Sphingomonadaceae* (*Alphaproteobacteria*), *Cytophagaceae* (*Cytophagia*), *Flavobacteriaceae* (*Flavobacteriia*), *Ellin6075* (*Chloracidobacteria*) were more abundant in DXAL(Fig. 7b). As for the reproductive growth stage, the relative abundance of *Proteobacteria*, *Acidobacteria*, *Bacteroidetes*, *Actinobacteria* and *Verrucomicrobia* were significantly different between two sites. We noted that most classes belonging to the *Proteobacteria*, were over-representation in LZ, such as *Rhizobiaceae* and *Beijerinckiaceae* (*Alphaproteobacteria*), *Xanthomonadaceae* (*Gammaproteobacteria*), *Oxalobacteraceae* and *Burkholderiaceae* (*BetaProteobacteria*), besides, *Acidobacteria*ceae (*Acidobacteriia*), and *Sphingobacteriaceae* (*Sphingobacteriia*) also more dominated in LZ; whereas *Comamonadaceae* (*Betaproteobacteria*), *Caulobacteraceae* (*Alphaproteobacteria*), *Bdellovibrionaceae* (*Deltaproteobacteria*), *Cytophagaceae* (*Cytophagia*), *Chitinophagaceae* (*Saprospirae*) were significantly enriched in DXAL.

Likewise, for the soil samples, the difference of bacterial community composition between two sites was shown in Additional file 2: Figure S3 and Additional file 1: Table

S12, at the vegetative growth stage, the dominant phyla were *Proteobacteria*, *Actinobacteria* and *Acidobacteria* (Additional file 2: Figure S3a). *Rhodospirillaceae* (*Alphaproteobacteria*), *Sinobacteraceae* (*Gammaproteobacteria*), *Gaiellaceae* (*Thermoleophilia*), *EB1017* and *C111* (*Acidimicrobiia*), *RB40* (*Acidobacteria-6*) were significantly enriched in LZ, whereas *Syntrophobacteraceae* and *Bdellovibrionaceae* (*Deltaproteobacteria*), *Sphingomonadaceae* (*Alphaproteobacteria*), *Ellin6075* (*Chloracidobacteria*) were over-present in DXAL (Additional file 2: Figure S3b); As for the reproductive growth stage, the different phyla was similar with vegetative growth stage (Additional file 2: Figure S3c), at the family level, the significantly different families were less, *Sinobacteraceae* and *Coxiellaceae* (*GammaProteobacteria*), *Koribacteraceae* (*Acidobacteriia*), *Solibacteraceae* (*Solibacteres*), *RB40* (*Acidobacteria-6*), *EB1017* (*Acidimicrobiia*), *Nocardioidaceae* (*Actinobacteria*) were dominant families in LZ soil bacterial core OTUs, only *Gaiellaceae* (*Thermoleophilia*) was significantly more enriched in DXAL (Additional file 2: Figure S3d). These results showed microbial composition differed between host biogeography, and common bacterial and fungal phyla were seen across each location that were broadly comparable to other plant hosts[25-27].

Comparative analyses of core microbiome across plant growth stages

The previous study revealed that the root-associated microbiomes has been shown to correlate with the developmental stage of the plant[28, 29]. To investigate the relationship between growth stage and the root-associated microbiome, two growth stages in two different growing regions were tested and compared. The difference of

fungal community compositions at the class level in the root and soil samples from two sites under two growth stages are shown in Fig. 8 and Additional file 1: Table S13. In LZ, taxonomic distributions of classes for the vegetative growth stage were overall similar to the reproductive growth stage: *Leotiomycetes* and *Agaricomycetes* make up the majority of the plant microbiota. The distribution of *Agaricomycetes*, *Eurotiomycetes*, *Mortierellomycetes* and *Pezizomycetes* significantly showed a decreasing trend from the vegetative growth stage to the reproductive growth stage in root samples, only *Orbiliomycetes* was showed an increasing trend (Fig. 8a). *Eurotiomycetes*, *Sordariomycetes*, *Dothideomycetes* and *Tremellomycetes* were enriched at vegetative growth stage in the soil compartment, while *Agaricomycetes*, *Glomeromycetes* and *Mortierellomycetes* were enriched at reproductive growth stage (Fig. 8b). As for DXAL, *Sordariomycetes* and *Mortierellomycetes* were over-present in vegetative growth stage in the root compartment, whereas *Leotiomycetes*, *Dothideomycetes* and *Eurotiomycetes* were over-present in reproductive growth stage (Fig. 8c). *Sordariomycetes* and *Tremellomycetes* were more dominant in vegetative growth stage in the soil compartment, whereas *Leotiomycetes*, *Agaricomycetes*, *Eurotiomycetes*, *Dothideomycetes* and *Mortierellomycetes* were highly persistent in reproductive growth stage (Fig. 8d).

For the difference of bacterial community composition between growth stage at two sites was shown in Fig. 9, Additional file 2: Figure S4 and Additional file 1: Table S14, the differential core OTUs involved phyla are almost similar at two sites in the root

353 compartment, such as *Proteobacteria*, *Acidobacteria*, *Verrucomicrobia*, *Chloroflexi*
354 and *TM7*, except *Bacteroidetes* and *Firmicutes* in LZ, and *Gemmatimonadetes* in
355 DXAL (Fig.9a, c). These dominate phyla were further analyzed at the family level. At
356 root samples, whether in LZ or DXAL, the relative abundance of most families was
357 higher in the reproductive growth stage, for example, *Rhizobiaceae*, *Rhodospirillaceae*
358 and *Caulobacteraceae* (*Alphaproteobacteria*), *Xanthomonadaceae* and
359 *Sinobacteraceae* (*Gammaproteobacteria*), *Comamonadaceae* (*Betaproteobacteria*),
360 *Sphingobacteriaceae* (*Sphingobacteriia*), at the vegetative growth stage,
361 *Hyphomicrobiaceae* (*Alphaproteobacteria*), *Ellin6075* (*Chloracidobacteria*),
362 *Chitinophagaceae* (*Saprospirae*), *Cytophagaceae* (*Cytophagia*) were more abundant in
363 LZ (Fig.9b), and *Flavobacteriaceae* (*Flavobacteriia*), *Ellin6075* (*Chloracidobacteria*)
364 were more prevent in DXAL (Fig.9d).
365
366 For the soil samples, the differential core OTUs involved phyla were similar like root
367 samples, but the significantly enriched families in three dominant phyla were different
368 from root, whether in LZ or DXAL, the relative abundance of most families was higher
369 in the vegetative growth stage (Additional file 2: Figure S4 and Additional file 1: Table
370 S14). The distribution of *Proteobacteria* generally showed a decreasing trend from the
371 vegetative growth stage to the reproductive growth stage in LZ (Additional file 2:
372 Figure S4a), included *Rhodospirillaceae* (*Alphaproteobacteria*), *Comamonadaceae*
373 (*Betaproteobacteria*), *Polyangiaceae* (*Deltaprotseobacteria*), in addition, *RB40*
374 (*Acidobacteria-6*), *EB1017*, *C111* (*Acidimicrobiia*), *Gaiellaceae* (*Thermoleophilia*),

Pseudonocardiaceae (*Actinobacteria*) were also significantly enriched in vegetative growth stage (Additional file 2: Figure S4b). Likewise, in the DXAL, *Comamonadaceae* (*Betaproteobacteria*), *Xanthomonadaceae* and *Coxiellaceae* (*Gammaproteobacteria*), *Ellin6075* (*Chloracidobacteria*), *Cytophagaceae* (*Cytophagia*), Saprospiraceae (*Saprospirae*) were over-present in vegetative growth stage, while *Rhodospirillaceae* (*Alphaproteobacteria*), *Syntrophobacteraceae* (*Deltaproteobacteria*), *Solibacteraceae* (*Solibacteres*), *Chitinophagaceae* (*Saprospirae*) were significantly enriched in reproductive growth stage (Additional file 2: Figure S4c, d). Consistent with previous observations, microbial composition differed between different development stages, it suggested that the overall recruitment of OTUs is governed by a set of factors that include developmental stage.

Discussion

In the present study, we performed geographical location and developmental stage study of the taxonomic features of *G. conopsea* root-associated microbiomes to better determine plant driven taxa and their properties in this habitat. Previous studies of root microbiomes have been mainly based on other orchids[19, 30-33]. The decreasing cost of amplicon sequencing approaches has made large-scale and global studies of microbiomes in possible. Recently, Chunsheng Hu, Binbin Liu and colleagues analyzed the root and rhizosphere microbiomes in wheat under the combined effect of plant development and nitrogen fertilization using a amplicon sequencing approach[34], their results indicate that both plant growth status and N input drive changes in the microbial community structure in the root zone of wheat. In this study, we analyzed the factors

affecting the composition of root-associated microbiomes using the amplicon sequencing approach. This is the first time that simultaneously examine the root-associated microbiomes that includes both fungi and bacteria in *G. conopsea*.

As revealed by the alpha diversity index, a significant differentiation of species diversity between bulk soils and root of *G. conopsea* was uncovered, which is in concordance with the general views of microbial colonization[35, 36]. Soil serves as one of the richest microbial ecosystems on Earth, providing ideal habitats for various microbial lineages[37]. The species diversity of plant compartments (root) was significantly lower, mainly owing to that, the process of microbial colonization and formation of stable communities in plant tissues was highly variable and more complex than expected, such as the host plant's innate immune system and their response to microbial colonization. The decrease of species diversity and richness from soil to plant root indicated that only a limited number of fungal/bacterial microbes could keep a symbiotic lifestyle with a host plant and finally become dominant root assemblages.

According to the PCoA analysis, remarkably variation of fungal/bacterial community structure was further disclosed regarding compartment, plant geographical location and developmental stage. The results uncovered that the key factor driving fungal/bacterial microbiome in *G. conopsea* plants were the geographical locations of the plant. This pattern was recapitulated by PERMANOVA based on UniFrac and Bray distances. Our result was consistent with the findings reported by Paloma Dura´n et al[35], in which

the host biogeography was the most important factor driving root fungal community composition. However, the result of bacterial microbiome was different from the study of other plant, such as rice[38], *Arabidopsis*[35], millet[10], *Cycas panzhihuaensis*[39] which suggested that the compartment was a larger source of variation than host biogeography and might be a major determining factor shaping the composition of the bacterial microbiome. It may have relationship with the characteristics of *G. conopsea* that it can grow at different habitats, such as the altitude from 265 m to 4700 m.

In this study, the samples were collected from two different altitude place approximately 5,466 kilometers away. Linzhi (LZ, 29°38′59″N/94°25′37″E) is in the southern part of Tibet , the altitude is 3600 m, and has a semi-humid tropical climate, whereas Greater Khingan Mountains (DXAL, 51°42′N/124°20′E) belongs to the north of Heilongjiang province, the altitude is 496 m and has a cold temperate continental monsoon climate. The variation of altitude and climate conditions, gave rise to the differentiation of local microbiomes, leading to the formation of distinct and highly diverse root-associated fungal/bacterial microbiota. LZ belongs to the region on the Qinghai–Tibet Plateau (QTP), which is also characterized by low oxygen, low temperature, reduced pathogen incidence, and high levels of UV radiation[40, 41]. For plants, the plateau environment of high altitude, low pressure, low oxygen, strong radiation is undoubtedly harsh plant growth. Due to its unique natural and geographical environment, the microbial composition of *G. conopsea* in Linzhi is of great value. As shown in the results, *Leotiomycetes*, *Agaricomycetes*, *Eurotiomycetes* and

441 *Mortierellomycetes* were more abundant in LZ core fungal OTUs than DXAL in both
442 root and soil samples at the vegetative growth stage, at family level, it includes
443 *Helotiaceae*, *Dermateaceae*, *Vibrisseaceae*, *Myxotrichaceae and Herpotrichiellaceae*,
444 which belongs to Dark septate endophytes (DSEs). DSE are facultative symbionts in
445 the phylum *Ascomycota* and widely distributed group of fungal root colonizers[42].
446 Previous researches revealed that DSE can improve plant growth, likely by way of
447 nitrogen mineralization and uptake and protection from pathogens[43-45], DSE have
448 also been shown to positively influence plant resistance to drought by increasing plant
449 growth, water and nutrient absorption, and/or facilitating plant resistance to oxidation
450 stress[46, 47]. Many studies have shown that the plants that can live in the plateau are
451 closely related to DSE, which can promote the growth of host plants and the absorption
452 of nutrients such as phosphorus[48, 49]. Arbuscular mycorrhiza (AM) is an ancient
453 mutualistic symbiosis between *Glomeromycota* fungi and many land plants, in which
454 fungi provide plants with nutrients acquired from the soil in exchange for carbohydrates
455 and lipids[50, 51]. In our results, *Ambisporaceae*, *Archaeosporaceae*, *Acaulosporaceae*,
456 *Gigasporaceae*, *Glomeraceae and Paraglomeraceae* significantly enriched in LZ soil
457 samples, most of these fungi are barely found in DXAL. It suggested that higher
458 altitudes are more conducive to AM growth. In addition, *Clavariaceae*, *Russulaceae*,
459 *Leotiaceae* and *Dictyosporiaceae* were more dominate in LZ root samples, whereas
460 these families were rare in DXAL root samples. These results indicated that these
461 fungal taxa may have important role for *G. conopsea* to adapt to high altitude
462 environment. Taken together, these results implied that each site contains a different

pool of fungal taxa and that the plant was not restricted to specific taxa but instead draws from available taxa in the pool to organize its microbiome. However, although the microbial composition varied greatly from LZ to DXAL, the dominant taxa were similar, and just the relative abundance of taxa was different, implying that the symbiotic microorganisms of *G. conopsea* still have certain specificity.

As for the bacterial communities, *Acidobacteria* and *Actinobacteria* were significantly abundant in LZ root samples at two developmental stages, while *Actinobacteria*, *Planctomycetes* and *TM7* were enriched in LZ soil samples at two developmental stages. *Actinobacteria* were enriched in LZ from both root and soil samples compared with DXAL. *Actinobacteria* are gram positive saprophytic bacteria and play an important role in plant development[52]. Moreover, *Actinobacteria* have strong colonization ability and can survive in various types of soil, and spore production which allows them to survive longer in various extreme conditions, such as irradiation, and drought[53-55]. *Acidobacteria* are abundant in diverse environments with active sulfur cycling[56-58], have the property that full functionality of the *Acidobacterial* dissimilatory sulfur pathways and degradation of cellulose produces acetic acid and hydrogen under anoxic condition[59, 60]. This result was consisting with the characteristics of bacteria and the special environment of LZ. In conclusion, we investigated association between *G. conopsea* root-associated microbiota composition and various factors including plant compartment, geographical location and developmental stage. The *G. conopsea* represent as an important model to study the associations between plants and microbial

communities across different geographical location, given their adaption to environments of different altitude. An intriguing result was that the plant geographical location was the most important factor driving root-associated community composition in both fungal and bacterial community structure. In addition, compartment and developmental stage should also be considered to analyze the variation of microbiota composition. Moreover, although the microbial composition varied greatly by the geographical location, the symbiotic microorganisms of *G. conopsea* still have certain specificity. The dominant microbiome of *G. conopsea* may benefit the host by nutrient supply and seedling growth, as well as adapt to different environment. Overall, this study provides a holistic understanding of microbiomes associated with different geographical location and developmental stage of *G. conopsea*. Hopefully, these efforts laying a foundation for harnessing the microbiome for sustainable *G. conopsea* production.

Conclusions

We observed the dynamics of *G. conopsea* root-associated fungal and bacterial communities from distinct biogeographical regions with significantly different altitudes in two growth stages at the same time for the first-time using amplicon sequencing approach. The richness of both fungal and bacterial communities was higher at the vegetative growth stage than reproductive growth stage in the root samples from two locations. The microbial community structure was significantly affected by locations with different altitudes, moreover, the developmental stage and compartment were also factors contributing to microbiome variation in *G. conopsea*. Some specific fungal and bacterial taxa were more abundant in *G. conopsea* from higher altitude location,

suggesting these microbes might be an important role for *G. conopsea* to adapt to high altitude environment. However, further investigations are needed to assess the variation in microbial community composition of root in *G. conopsea* via different growth locations, such as collecting samples from more location with different altitudes. Overall, this study provides a holistic understanding of microbiomes associated with different locations and growth stages of an orchid species. Hopefully, these efforts laying a foundation for harnessing the microbiome for sustainable *G. conopsea* production.

Methods

Microbiome sample collection

Representative *Gymnadenia conopsea* (L.) R. Br. root and corresponding soil samples were collected uniformly from the natural habitats at Linzhi (29°38′59″N/94°25′37″E, Tibet, China) and Greater Khingan Mountains (51°42′N/124°20′E, Heilongjiang, China) using the following protocol. The root and soil were sampled two times in Linzhi and Greater Khingan Mountains, corresponding to two growth stages of plant: vegetative growth stage and reproductive growth stage. Fourteen individual plants were sampled from two locations for the root and corresponding bulk soil samples. Plant individuals were dug out with their surrounding soil, transferred into sterile a plastic bag and transported on ice to the laboratory. The soil samples were collected at a depth of 5-10 cm below plant growing ground level and surrounding plant approximately 5-cm diameter, the soil samples were sieved with 2 mm mesh to remove visible impurities such as fine roots and large organic debris and are defined as the soil fraction. The

corresponding bulk soil of each plant were sampled five biological replicates. The roots were manually separated from the soil and then gently shaken to remove the adhering soil particles. The roots were cut into small sections of 2-3 cm and thoroughly washed using sterile water to remove visible soil particles, and then washed successively in 75% ethanol, 0.25% NaOCl to further clean the root surfaces from living microorganisms and finally washed three times in sterile water. These step roots were defined as microbially-enriched root fraction. These treated soil and root samples were transferred to 2 mL tubes. All the samples were stored at 80 °C until DNA extraction. In total, 70 soil samples and 75 root samples were obtained from 2 representative locations in China.

DNA extraction and sequencing for 16S rRNA gene and ITS2 gene

Total DNA was extracted from the aforementioned samples using the NucleoSpin Soil Kit (Macherey-Nagel GmbH & Co.KG - Düren, Germany) according to the manufacturer's instructions. The DNA quality and quantity were assessed using a NanoDrop device (Thermo Scientific, Wilmington, DE) and electrophoresis (1% agarose gel, including a 1 kb plus ladder). All the qualified DNA were used to construct libraries. All samples were carried out by sequencing the V3-V4 region of bacterial 16S rRNA gene (341F-806R) and the ITS3- ITS4 region of fungal ITS2 gene. These primers were designed to amplify target sequence and they include dual index and adapters for annealing to the Illumina Miseq flow cell. In both cases, only the qualified library can be used for sequencing. After quality control, quantification and normalization of the DNA libraries, 300-bp paired-end reads were generated from MiSeq platform (BGI-Shenzhen, Shenzhen, China) for the amplicon (16S rRNA and ITS2 gene) analyses,

552 respectively[61].

553 **Amplicon sequence processing and analyses**

554 Microbial community composition was determined by sequencing 16S rRNA and
555 ITS2 gene amplicons from DNA samples from the *Gymnadenia conopsea* (L.) R. Br.
556 root and corresponding bulk soil. The high-quality paired-end reads of the 16S rRNA
557 gene V3-V4 region and ITS2 gene were merged using FLASH software with the
558 default setting[62]. The operational taxonomic units (OTUs) were clustered using the
559 UPARSE algorithm[63] at 97% sequence identity along with filtering the chimeras by
560 UCHIME[64]. To obtain the taxonomic information of the OTUs, the original reads
561 were assigned back to their OTUs using the USEARCH global alignment
562 algorithm[65], the representative sequences of each OTU were generated and aligned
563 against the Greengenes (v13_8 release/2013_5_99) and UNITE (2019_version8)
564 reference databases using the Ribosomal Database Project (RDP) classifier[66] for
565 bacterial and fungal communities, respectively. OTUs classified as mitochondria or
566 chloroplast, or less than 5 sequences, were filtered from the datasets.

567 **Diversity analysis**

568 Within-sample diversity (alpha-diversity) was calculated for each sample by Chao and
569 Shannon indices using mothur [67] from the final OTU table. Boxplot were plotted
570 using R software. The significant differences in alpha diversity from different groups
571 were determined using the Kruskal-Wallis and Dunn's post hoc tests (krus.test in R, p
572 < 0.05). To estimate beta-diversity, OTU table was normalized by the cumulative sum
573 scaling (CSS) method[68]. Bray-Curtis, unweighted UniFrac, and Weighted UniFrac

distances between samples were calculated from the normalized OTU table. The taxonomic dissimilarity analysis between samples was performed based on principal coordinate analysis (PCoA, cmdscale function in R) based on Bray-Curtis, weighted UniFrac (WUF) and unweighted UniFrac (UUF). The UniFrac distance is based on taxonomic relatedness, where the weighted UniFrac (WUF) metric takes abundance of taxa into consideration whereas the unweighted UniFrac (UUF) based on shared membership and is thus more sensitive to rare taxa. To assess the influence of the different factors (site, compartment and stage) on the beta diversity, permutation multivariate analysis of variance (PERMANOVA) analysis was performed (Adonis function from vegan package, in R).

Significantly Differential Core OTUs analysis

OTUs with occurrence frequency greater than 90% in the root or soil samples from each group were referred to here as "core OTUs." To identify significantly differential core OTUs between each pair of groups that need to compare, the Wilcoxon signed rank test was implemented among core OTUs in each group, with relative abundance considered separately in each sample. The P values of these tests were corrected for multiple testing using the Benjamini and Hochberg (BH) method. The core OTUs enriched in each group (adjusted $P < 0.05$) were then defined as "differential core OTUs". The comparison of core taxa of the root/soil microbiome between each pair of groups were based on differential core OTUs.

Microbial function prediction

We used FUNGuild[69] to classify each core OTU into an ecological guild to determine

596 if fungal functional groups differed in relative abundance between host biogeography
597 within compartment (root, soil) at two developmental stages. Core OTUs identified to
598 a guild with a confidence ranking of "highly probable" or "probable" were retained for
599 further analysis, whereas those with "possible" were removed. Bacteria microbial
600 function prediction was performed using the PICRUSt software[69]. Differentially
601 enriched KO pathways or modules were identified according to their reporter score
602 from the Z-scores of individual KOs. One-tail Wilcoxon rank-sum test was performed
603 on all the KOs and adjusted for multiple testing using the Benjamin–Hochberg
604 procedure. The Z-score for each KO could then be calculated. Absolute value of
605 reporter score ≥ 1.96 (95% confidence on either tail, according to normal distribution)
606 could be used as a detection threshold for significantly differentiating pathways.
607

608 **Acknowledgements**

609 We gratefully acknowledge Weiwu Chen, Jiumei Ciwang and Qunfang Wan for their
610 help with sampling. We also thank friends at BGI-Shenzhen for DNA extraction, library
611 construction, sequencing, and discussions.

612 **Authors' contributions**

613 Z.M. conceived and supervised the project. M.L. collected samples and designed the
614 experiment. M.L. and L.L. analyzed the data. H.X., X.X. and Z.Z. helped with sample
615 treatment. L.L. provided comments and suggests on the results. M.L. wrote and revised
616 the manuscript. All authors read and approved the final manuscript.

Funding

This research was supported by the National Major Scientific and Technological Special Project for "Significant New Drugs Development" of China (No. 2017ZX09301060) and National Key Research and Development Program of China (No. 2018YFC1708004).

Availability of data and material

The raw sequencing reads were deposited in the NCBI Bioproject database under the accession number PRJNA598558 (ITS data) and PRJNA598739 (16S data). Other data supporting the findings of the study are available in this article and its Supplementary Information files.

Ethics approval and consent to participate

Not applicable.

Consent for publication

Not applicable.

Competing interests

The authors declare that they have no competing interests.

References

1. Yuan J, Zhao J, Wen T, Zhao M, Li R, Goossens P, Huang Q, Bai Y, Vivanco JM, Kowalchuk GA et al. Root exudates drive the soil-borne legacy of aboveground pathogen infection. Microbiome. 2018; 6(1): 156.
2. Qin Y, Druzhinina IS, Pan X, Yuan Z. Microbially Mediated Plant Salt Tolerance and Microbiome-based Solutions for Saline Agriculture. Biotechnol. Adv. 2016; 34(7): 1245-59.
3. Berendsen RL, Pieterse CM, Bakker PA. The rhizosphere microbiome and plant health. Trends Plant Sci. 2012; 17(8): 478-86.
4. Ettema CH, Wardle DA. Spatial soil ecology. Trends Ecol. Evol. 2002; 17(4): 177-83.
5. Turner TR, James EK, Poole PS. The plant microbiome. Genome Biol. 2013; 14(6): 209.

643 6. Bai Y, Muller DB, Srinivas G, Garrido-Oter R, Potthoff E, Rott M, Dombrowski N, Munch PC,
644 Spaepen S, Remus-Emsermann M et al. Functional overlap of the Arabidopsis leaf and root
645 microbiota. Nature. 2015; 528(7582): 364-9.
646 7. Lundberg DS, Lebeis SL, Paredes SH, Yourstone S, Gehring J, Malfatti S, Tremblay J,
647 Engelbrektson A, Kunin V, Del RT et al. Defining the core Arabidopsis thaliana root microbiome.
648 Nature. 2012; 488(7409): 86-90.
649 8. Sessitsch A, Hardoim P, Doring J, Weilharter A, Krause A, Woyke T, Mitter B, Hauberg-Lotte L,
650 Friedrich F, Rahalkar M et al. Functional characteristics of an endophyte community colonizing rice
651 roots as revealed by metagenomic analysis. Mol Plant Microbe Interact. 2012; 25(1): 28-36.
652 9. Peiffer JA, Spor A, Koren O, Jin Z, Tringe SG, Dangl JL, Buckler ES, Ley RE. Diversity and
653 heritability of the maize rhizosphere microbiome under field conditions. Proc Natl Acad Sci U S A.
654 2013; 110(16): 6548-53.
655 10. Jin T, Wang Y, Huang Y, Xu J, Zhang P, Wang N, Liu X, Chu H, Liu G, Jiang H et al. Taxonomic
656 structure and functional association of foxtail millet root microbiome. Gigascience. 2017; 6(10): 1-
657 12.
658 11. Cregger MA, Veach AM, Yang ZK, Crouch MJ, Vilgalys R, Tuskan GA, Schadt CW. The Populus
659 holobiont: dissecting the effects of plant niches and genotype on the microbiome. Microbiome. 2018;
660 6(1): 31.
661 12. Xu J, Zhang Y, Zhang P, Trivedi P, Riera N, Wang Y, Liu X, Fan G, Tang J, Coletta-Filho HD et
662 al. The structure and function of the global citrus rhizosphere microbiome. Nat Commun. 2018;
663 9(1): 4894.
664 13. Hultén E, Fries M: Atlas of North European vascular plants (North of the Tropic of Cancer).
665 Germany: Koeltz Scientific Books; 1986.
666 14. McCormick MK, Jacquemyn H. What constrains the distribution of orchid populations? New Phytol.
667 2014; 202(2): 392-400.
668 15. Curtis JT. The relation of specificity of orchid mycorrhizal fungi to the problem of symbiosis. Am.
669 J. Bot. 1939; 26(6): 390-9.
670 16. Perkins A, Masuhara G, McGee PA. Specificity of the Associations Between Microtis parviflora
671 (Orchidaceae) and Its Mycorrhizal Fungi. Aust. J. Bot. 1995; 43(1): 85-91.
672 17. Masuhara G, Katsuya K. In situ and In vitro Specificity between Rhizoctonia spp. and Spiranthes

673 sinensis (Persoon) Ames. var. amoena (M. Bieberstein) Hara (Orchidaceae). New Phytologist. 1994;
674 127(4): 711-8.
675 18. McCormick MK, Whigham DF, Canchani-Viruet A. Mycorrhizal fungi affect orchid distribution
676 and population dynamics. New Phytol. 2018; 219(4): 1207-15.
677 19. Voyron S, Ercole E, Ghignone S, Perotto S, Girlanda M. Fine-scale spatial distribution of orchid
678 mycorrhizal fungi in the soil of host-rich grasslands. New Phytol. 2017; 213(3): 1428-39.
679 20. Taylor DL, McCormick MK. Internal transcribed spacer primers and sequences for improved
680 characterization of basidiomycetous orchid mycorrhizas. New Phytol. 2008; 177(4): 1020-33.
681 21. Kristiansen KA, Taylor DL, Kjoller R, Rasmussen HN, Rosendahl S. Identification of mycorrhizal
682 fungi from single pelotons of Dactylorhiza majalis (Orchidaceae) using single-strand
683 conformation polymorphism and mitochondrial ribosomal large subunit DNA sequences. Mol. Ecol.
684 2001; 10(8): 2089-93.
685 22. Tsavkelova EA, Cherdyntseva TA, Botina SG, Netrusov AI. Bacteria associated with orchid roots
686 and microbial production of auxin. Microbiol. Res. 2007; 162(1): 69-76.
687 23. Shade A, Handelsman J. Beyond the Venn diagram: the hunt for a core microbiome. Environ.
688 Microbiol. 2012; 14(1): 4-12.
689 24. van der Heijden MG, de Bruin S, Luckerhoff L, van Logtestijn RS, Schlaeppi K. A widespread
690 plant-fungal-bacterial symbiosis promotes plant biodiversity, plant nutrition and seedling
691 recruitment. Isme J. 2016; 10(2): 389-99.
692 25. Peay KG, Kennedy PG, Talbot JM. Dimensions of biodiversity in the Earth mycobiome. Nat. Rev.
693 Microbiol. 2016; 14(7): 434-47.
694 26. Pinto C, Pinho D, Sousa S, Pinheiro M, Egas C, Gomes AC. Unravelling the diversity of grapevine
695 microbiome. Plos One. 2014; 9(1): e85622.
696 27. Ottesen AR, Gonzalez PA, White JR, Pettengill JB, Li C, Allard S, Rideout S, Allard M, Hill T,
697 Evans P et al. Baseline survey of the anatomical microbial ecology of an important food plant:
698 Solanum lycopersicum (tomato). Bmc Microbiol. 2013; 13: 114.
699 28. Lundberg DS, Lebeis SL, Paredes SH, Yourstone S, Gehring J, Malfatti S, Tremblay J,
700 Engelbrektson A, Kunin V, Del RT et al. Defining the core Arabidopsis thaliana root microbiome.
701 Nature. 2012; 488(7409): 86-90.
702 29. Skaltsas DN, Badotti F, Vaz A, Silva F, Gazis R, Wurdack K, Castlebury L, Goes-Neto A, Chaverri

703 P. Exploration of stem endophytic communities revealed developmental stage as one of the drivers
704 of fungal endophytic community assemblages in two Amazonian hardwood genera. Sci Rep. 2019;
705 9(1): 12685.
706 30. Fochi V, Chitarra W, Kohler A, Voyron S, Singan VR, Lindquist EA, Barry KW, Girlanda M,
707 Grigoriev IV, Martin F et al. Fungal and plant gene expression in the Tulasnella calospora-Serapias
708 vomeracea symbiosis provides clues about nitrogen pathways in orchid mycorrhizas. New Phytol.
709 2017; 213(1): 365-79.
710 31. Xing X, Gai X, Liu Q, Hart MM, Guo S. Mycorrhizal fungal diversity and community composition
711 in a lithophytic and epiphytic orchid. Mycorrhiza. 2015; 25(4): 289-96.
712 32. Selosse MA, Martos F. Do chlorophyllous orchids heterotrophically use mycorrhizal fungal carbon?
713 Trends Plant Sci. 2014; 19(11): 683-5.
714 33. Leake JR, Cameron DD. Untangling above- and belowground mycorrhizal fungal networks in
715 tropical orchids. Mol. Ecol. 2012; 21(20): 4921-4.
716 34. Chen S, Waghmode TR, Sun R, Kuramae EE, Hu C, Liu B. Root-associated microbiomes of wheat
717 under the combined effect of plant development and nitrogen fertilization. Microbiome. 2019; 7(1):
718 136.
719 35. Duran P, Thiergart T, Garrido-Oter R, Agler M, Kemen E, Schulze-Lefert P, Hacquard S. Microbial
720 Interkingdom Interactions in Roots Promote Arabidopsis Survival. Cell. 2018; 175(4): 973-83.
721 36. Beckers B, Op DBM, Weyens N, Boerjan W, Vangronsveld J. Structural variability and niche
722 differentiation in the rhizosphere and endosphere bacterial microbiome of field-grown poplar trees.
723 Microbiome. 2017; 5(1): 25.
724 37. Wei N, Ashman TL. The effects of host species and sexual dimorphism differ among root, leaf and
725 flower microbiomes of wild strawberries in situ. Sci Rep. 2018; 8(1): 5195.
726 38. Edwards J, Johnson C, Santos-Medellin C, Lurie E, Podishetty NK, Bhatnagar S, Eisen JA,
727 Sundaresan V. Structure, variation, and assembly of the root-associated microbiomes of rice. Proc
728 Natl Acad Sci U S A. 2015; 112(8): E911-20.
729 39. Zheng Y, Gong X. Niche differentiation rather than biogeography shapes the diversity and
730 composition of microbiome of Cycas panzhihuaensis. Microbiome. 2019; 7(1): 152.
731 40. Qiao Q, Huang Y, Qi J, Qu M, Jiang C, Lin P, Li R, Song L, Yonezawa T, Hasegawa M et al. The
732 genome and transcriptome of Trichormus sp. NMC-1: insights into adaptation to extreme

environments on the Qinghai-Tibet Plateau. Sci Rep. 2016; 6: 29404.

41. Qiao Q, Wang Q, Han X, Guan Y, Sun H, Zhong Y, Huang J, Zhang T. Transcriptome sequencing of Crucihimalaya himalaica (Brassicaceae) reveals how Arabidopsis close relative adapt to the Qinghai-Tibet Plateau. Sci Rep. 2016; 6: 21729.
42. Rodriguez RJ, White JJ, Arnold AE, Redman RS. Fungal endophytes: diversity and functional roles. New Phytol. 2009; 182(2): 314-30.
43. Mullen RB, Schmidt SK, Jaeger CH. Nitrogen Uptake during Snowmelt by the Snow Buttercup, Ranunculus adoneus. Arctic and Alpine Research. 1998; 30(2): 121-5.
44. Mandyam K, Jumpponen A. Seeking the elusive function of the root-colonising dark septate endophytic fungi. Stud. Mycol. 2005; 53: 173-89.
45. Newsham KK. A meta-analysis of plant responses to dark septate root endophytes. New Phytol. 2011; 190(3): 783-93.
46. Santos S, Silva P, Garcia AC, Zilli JE, Berbara R. Dark septate endophyte decreases stress on rice plants. Braz. J. Microbiol. 2017; 48(2): 333-41.
47. Perez-Naranjo, Juan, Carlos: Dark Septate and Arbuscular Mycorrhizal Fungal Endophytes in Roots of Prairie Grasses. Saskatchewan: The University of Saskatchewan; 2009.
48. Jumpponen A. Dark septate endophytes - Are they mycorrhizal? Mycorrhiza. 2001; 11(4): 207-11.
49. Jumpponen A, Mattson KG, Trappe JM. Mycorrhizal functioning of Phialocephala fortinii with Pinus contorta on glacier forefront soil: interactions with soil nitrogen and organic matter. Mycorrhiza. 1998; 7(5): 261-5.
50. Rich MK, Nouri E, Courty P, Reinhardt D. Diet of Arbuscular Mycorrhizal Fungi: Bread and Butter? Trends Plant Sci. 2017; 22(8): 652-60.
51. Delaux PM, Radhakrishnan GV, Jayaraman D, Cheema J, Malbreil M, Volkening JD, Sekimoto H, Nishiyama T, Melkonian M, Pokorny L et al. Algal ancestor of land plants was preadapted for symbiosis. Proc Natl Acad Sci U S A. 2015; 112(43): 13390-5.
52. Verma VC, Gond SK, Kumar A, Mishra A, Kharwar RN, Gange AC. Endophytic actinomycetes from Azadirachta indica A. Juss.: isolation, diversity, and anti-microbial activity. Microb. Ecol. 2009; 57(4): 749-56.
53. Palaniyandi SA, Yang SH, Zhang L, Suh JW. Effects of actinobacteria on plant disease suppression and growth promotion. Appl Microbiol Biotechnol. 2013; 97(22): 9621-36.

763 54. Yandigeri MS, Meena KK, Singh D, Malviya N, Singh DP. Drought-tolerant endophytic
764 actinobacteria promote growth of wheat (Triticum aestivum) under water stress conditions. Plant
765 Growth Regul. 2012; 68(3): 411-20.
766 55. Qin S, Xing K, Jiang JH, Xu LH, Li WJ. Biodiversity, bioactive natural products and
767 biotechnological potential of plant-associated endophytic actinobacteria. Appl Microbiol
768 Biotechnol. 2011; 89(3): 457-73.
769 56. Urbanova Z, Barta J. Microbial community composition and in silico predicted metabolic potential
770 reflect biogeochemical gradients between distinct peatland types. Fems Microbiol. Ecol. 2014;
771 90(3): 633-46.
772 57. Serkebaeva YM, Kim Y, Liesack W, Dedysh SN. Pyrosequencing-based assessment of the bacteria
773 diversity in surface and subsurface peat layers of a northern wetland, with focus on poorly studied
774 phyla and candidate divisions. Plos One. 2013; 8(5): e63994.
775 58. Sanchez-Andrea I, Rodriguez N, Amils R, Sanz JL. Microbial diversity in anaerobic sediments at
776 Rio Tinto, a naturally acidic environment with a high heavy metal content. Appl Environ Microbiol.
777 2011; 77(17): 6085-93.
778 59. Hausmann B, Pelikan C, Herbold CW, Kostlbacher S, Albertsen M, Eichorst SA, Glavina DRT,
779 Huemer M, Nielsen PH, Rattei T et al. Peatland Acidobacteria with a dissimilatory sulfur
780 metabolism. Isme J. 2018; 12(7): 1729-42.
781 60. Pankratov TA, Kirsanova LA, Kaparullina EN, Kevbrin VV, Dedysh SN. Telmatobacter bradus gen.
782 nov., sp. nov., a cellulolytic facultative anaerobe from subdivision 1 of the Acidobacteria, and
783 emended description of Acidobacterium capsulatum Kishimoto et al. 1991. Int J Syst Evol
784 Microbiol. 2012; 62(Pt 2): 430-7.
785 61. Fadrosh DW, Ma B, Gajer P, Sengamalay N, Ott S, Brotman RM, Ravel J. An improved dual-
786 indexing approach for multiplexed 16S rRNA gene sequencing on the Illumina MiSeq platform.
787 Microbiome. 2014; 2(1): 6.
788 62. Magoc T, Salzberg SL. FLASH: fast length adjustment of short reads to improve genome assemblies.
789 Bioinformatics. 2011; 27(21): 2957-63.
790 63. Edgar RC. UPARSE: highly accurate OTU sequences from microbial amplicon reads. Nat. Methods.
791 2013; 10(10): 996-8.
792 64. Edgar RC, Haas BJ, Clemente JC, Quince C, Knight R. UCHIME improves sensitivity and speed

of chimera detection. Bioinformatics. 2011; 27(16): 2194-200.

65. Edgar RC. Search and clustering orders of magnitude faster than BLAST. Bioinformatics. 2010; 26(19): 2460-1.

66. Wang Q, Garrity GM, Tiedje JM, Cole JR. Naive Bayesian classifier for rapid assignment of rRNA sequences into the new bacterial taxonomy. Appl Environ Microbiol. 2007; 73(16): 5261-7.

67. Schloss PD, Westcott SL, Ryabin T, Hall JR, Hartmann M, Hollister EB, Lesniewski RA, Oakley BB, Parks DH, Robinson CJ et al. Introducing mothur: open-source, platform-independent, community-supported software for describing and comparing microbial communities. Appl Environ Microbiol. 2009; 75(23): 7537-41.

68. Paulson JN, Stine OC, Bravo HC, Pop M. Differential abundance analysis for microbial marker-gene surveys. Nat. Methods. 2013; 10(12): 1200-2.

69. Nguyen NH, Song Z, Bates ST, Branco S, LehoTedersoo, Menke J, S. J, Schilling, Kennedy PG. FUNGuild: An open annotation tool for parsing fungal community datasets by ecological guild. Fungal Ecol. 2016; 20: 241-8.

Figure legend

Fig. 1 Species richness and diversity of root-associated microbial communities. **a** Microbial richness index comparison between each group based on the Chao index using the ITS data. **b** Microbial diversity index comparison between each group based on the Shannon index using the ITS data. **c** Microbial richness index comparison between each group based on the Chao index using the 16S rRNA gene data. **d** Microbial diversity index comparison between each group based on the Shannon index using the 16S rRNA gene data. Significant differences are depicted with letters ($p < 0.05$, Kruskal-Wallis with Dunn's post hoc test). DXAL: Greater Khingan Mountains, LZ: Linzhi, 1: vegetative growth stage, 2: reproductive growth stage

Fig. 2 Principal coordinate analyses (PCoAs) of microbial community composition among different sample types of *G. conopsea*. **a** PCoA using the weighted UniFrac

(WUF) distances at the OTU level using fungal community's data**. b** PCoA using the unweighted UniFrac (UUF) distances at the OTU level using fungal community's data. **c** PCoA using the weighted UniFrac (WUF) distances at the OTU level using bacterial community's data**. d** PCoA using the unweighted UniFrac (UUF) distances at the OTU level using bacterial community's data. Samples are color coded according to the sites, compartments, and developmental stages are depicted with different symbols. DXAL: Greater Khingan Mountains, LZ: Linzhi, 1: vegetative growth stage, 2: reproductive growth stage

Fig. 3 Microbial community composition among different sample types of *G. conopsea* at phylum level. **a** Relative abundance of fungal taxa of each group. **b** Relative abundance of bacterial taxa of each group. DXAL: Greater Khingan Mountains, LZ: Linzhi, 1: vegetative growth stage, 2: reproductive growth stage

Fig. 4 Compositions of fungal functional group (guild) inferred by FUNGuild. **a** At the trophic mode level. **b** At guilds level. **c** At Growth_Morphology level. DXAL: Greater Khingan Mountains, LZ: Linzhi, 1: vegetative growth stage, 2: reproductive growth stage

Fig. 5 Alterations in bacteria microbial functional modules in each compare group. Dashed lines indicate a reporter score of 1.96, corresponding to 95% confidence in a normal distribution**.** DXAL_1: DXAL_1_Root vs DXAL_1_Soil, DXAL_2: DXAL_2_Root vs DXAL_2_Soil, LZ_1: LZ_1_Root vs LZ_1_Soil, LZ_2: LZ_2_Root vs LZ_2_Soil. DXAL: Greater Khingan Mountains, LZ: Linzhi, 1: vegetative growth stage, 2: reproductive growth stage

842 **Fig. 6** Side-by-side comparison of the relative abundance (‰) of classes which made
843 up at least >10‰ of the total fungal core microbiome community across different sites.
844 **a** Relative abundance (‰) of the classes detected in root core OTUs of the indicated
845 plant growth sites at vegetative growth stage. **b** Relative abundance (‰) of the classes
846 detected in soil core OTUs of the indicated plant growth sites at vegetative growth stage.
847 **c** Relative abundance (‰) of the classes detected in root core OTUs of the indicated
848 plant growth sites at reproductive growth stage. **d** Relative abundance (‰) of the
849 classes detected in soil core OTUs of the indicated plant growth sites at reproductive
850 growth stage. Asterisks indicate significant differences occur between Linzhi and
851 Greater Khingan Mountains (Benjamini–Hochberg false discovery-rate (FDR) adjusted
852 P value, * represent < 0.05, ** represent < 0.01, *** represent < 0.001) in each
853 compartment.
854 **Fig. 7** Comparative analyses of bacterial core microbiome across different sites. **a**
855 Relative abundance (‰) of the phyla detected in root core OTUs of the indicated plant
856 growth sites at vegetative growth stage. **b** Relative abundance (‰ of families belonging
857 to the three dominant phyla in the root core OTUs of the indicated plant growth sites at
858 vegetative growth stage. **c** Relative abundance (‰) of the phyla detected in root core
859 OTUs of the indicated plant growth sites at reproductive growth stage. **d** Relative
860 abundance (‰ of families belonging to the three dominant phyla in the root core OTUs
861 of the indicated plant growth sites at reproductive growth stage. Asterisks indicate
862 significant differences (Benjamini–Hochberg false discovery-rate (FDR) adjusted P
863 value, * represent < 0.05, ** represent < 0.01, *** represent < 0.001).

Fig. 8 Side-by-side comparison of the relative abundance (‰) of classes which made up at least >10‰ of the total fungal core microbiome community across different developmental stages. **a** Relative abundance (‰) of the classes detected in root core OTUs of the indicated developmental stages in Linzhi. **b** Relative abundance (‰) of the classes detected in soil core OTUs of the indicated plant growth sites in Linzhi. **c** Relative abundance (‰) of the classes detected in root core OTUs of the indicated plant growth sites in Greater Khingan Mountains. **d** Relative abundance (‰) of the classes detected in soil core OTUs of the indicated plant growth sites in Greater Khingan Mountains. Asterisks indicate significant differences occur between vegetative growth stage and reproductive growth stage (Benjamini–Hochberg false discovery-rate (FDR) adjusted P value, * represent < 0.05, ** represent < 0.01, *** represent < 0.001) in each compartment.

Fig. 9 Comparative analyses of bacterial core microbiome across different developmental stages. **a** Relative abundance (‰) of the phyla detected in root core OTUs of the indicated developmental stages in Linzhi. **b** Relative abundance (‰ of families belonging to the three dominant phyla in the root core OTUs of the indicated developmental stages in Linzhi. **c** Relative abundance (‰) of the phyla detected in root core OTUs of the indicated plant growth sites in Greater Khingan Mountains. **d** Relative abundance (‰ of families belonging to the three dominant phyla in the root core OTUs of the indicated plant growth sites in Greater Khingan Mountains. Asterisks indicate significant differences (Benjamini–Hochberg false discovery-rate (FDR) adjusted P value, * represent < 0.05, ** represent < 0.01, *** represent < 0.001).

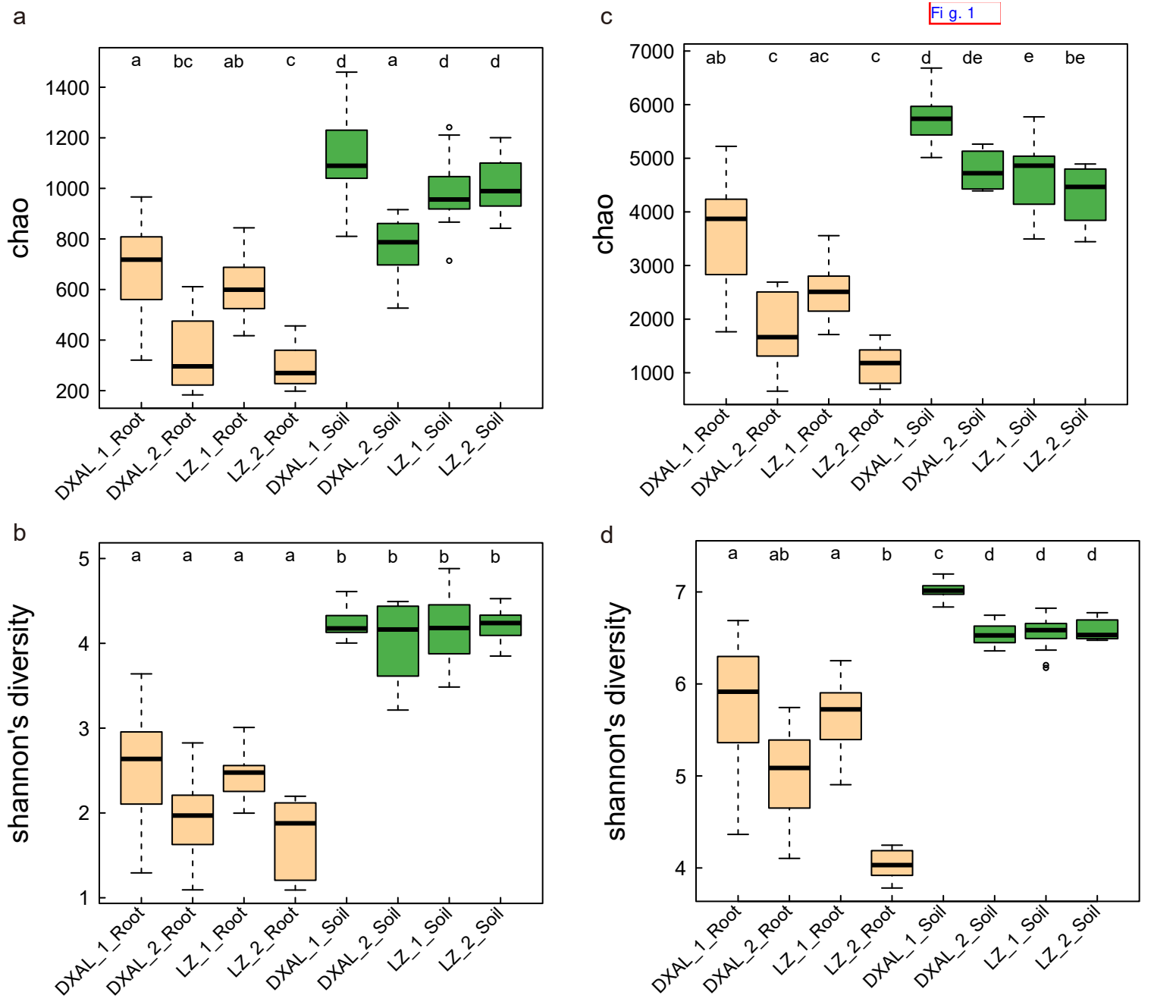
a
chao
1400
1200
1000
800
600
400
200
a bc ab c d a d d
DXAL_1_Root
DXAL_2_Root
LZ_1_Root
LZ_2_Root
DXAL_1_Soil
DXAL_2_Soil
LZ_1_Soil
LZ_2_Soil
c
Fi g. 1
chao
7000
6000
5000
4000
3000
2000
1000
ab c ac c d de e be
b
shannon's diversity
5
4
3
2
1
a a a a b b b b
d
shannon's diversity
7
6
5
4
a ab a b c d d d

Fi g. 2

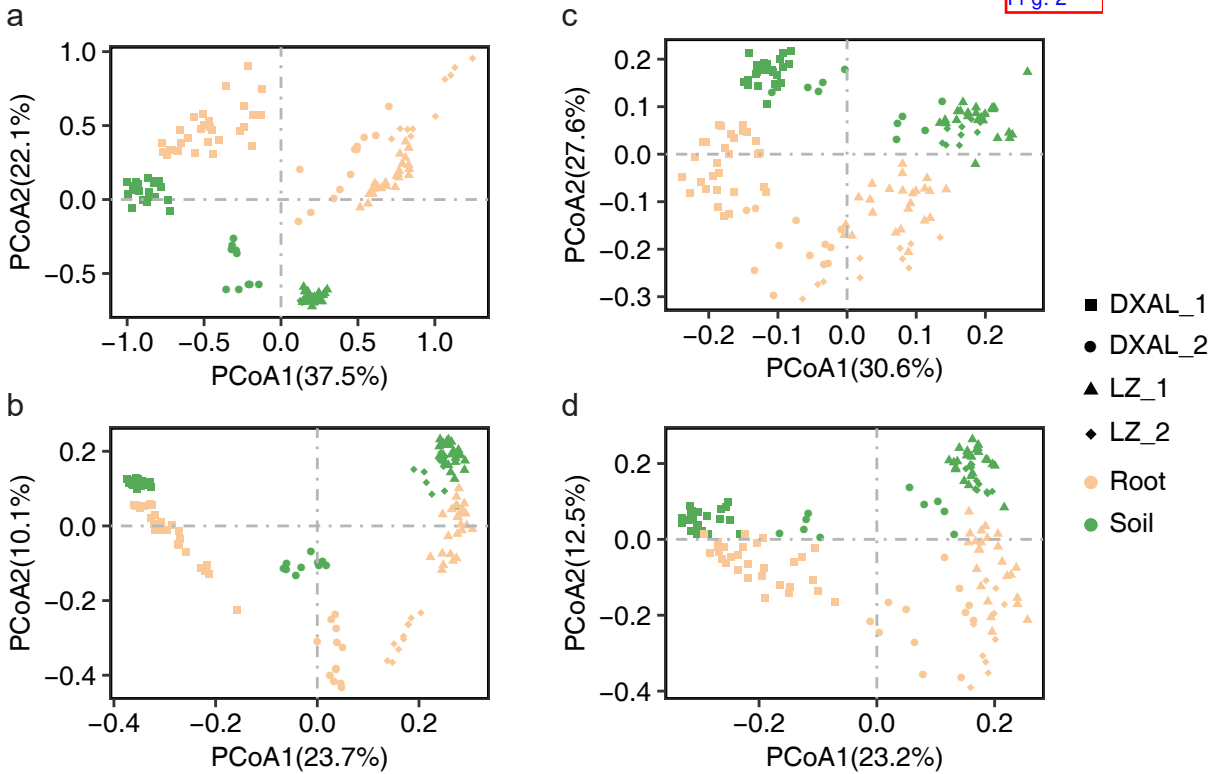
a
PCoA2(22.1%)
PCoA1(37.5%)
b
PCoA2(10.1%)
PCoA1(23.7%)
c
PCoA2(27.6%)
PCoA1(30.6%)
d
PCoA2(12.5%)
PCoA1(23.2%)
DXAL_1
DXAL_2
LZ_1
LZ_2
Root
Soil

Fi g. 3

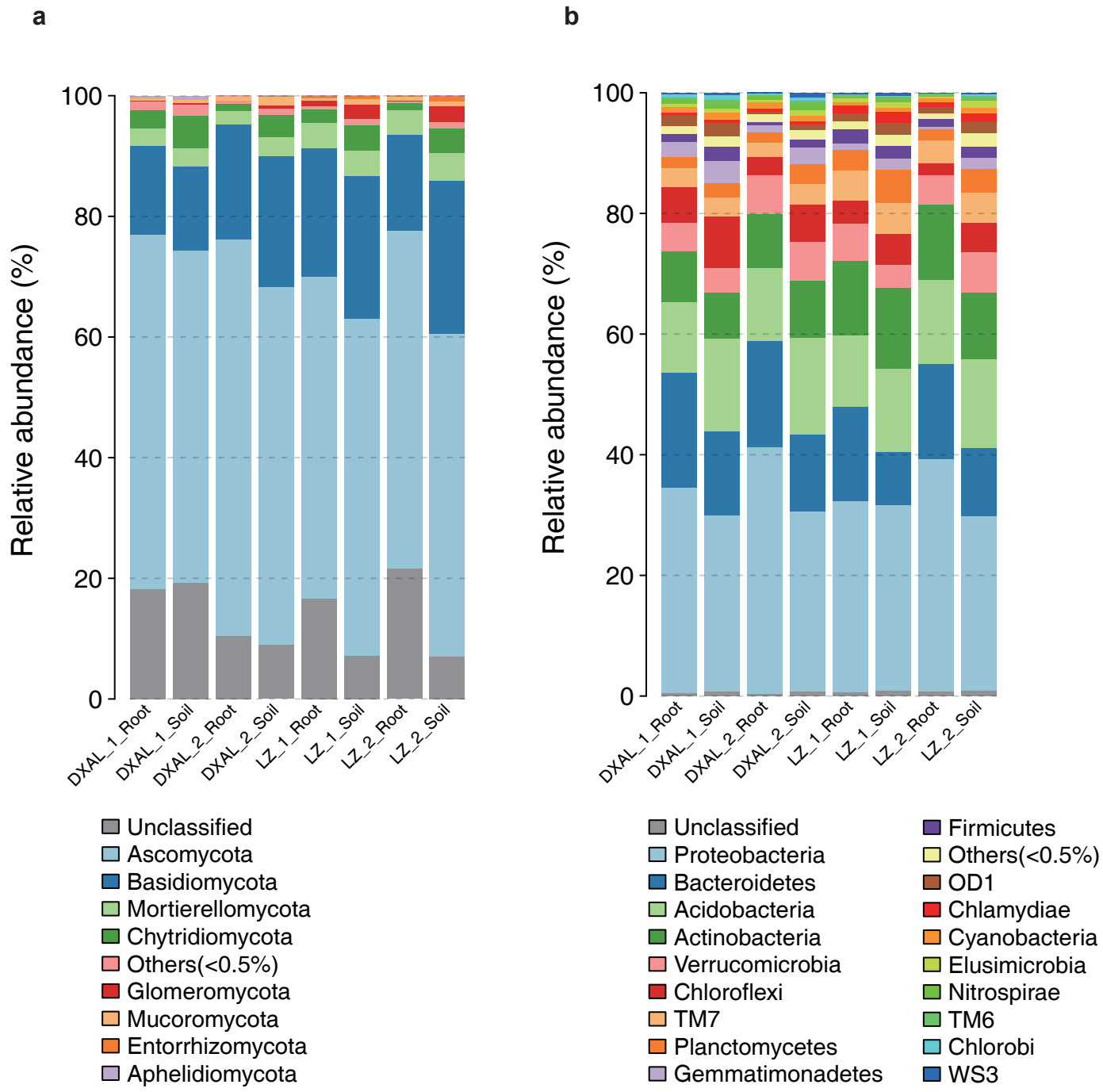
a
b
Relative abundance (%)
100
80
60
40
20
0
DXAL_1_Root
DXAL_1_Soil
DXAL_2_Root
DXAL_2_Soil
LZ_1_Root
LZ_1_Soil
LZ_2_Root
LZ_2_Soil
Unclassified
Ascomycota
Basidiomycota
Mortierellomycota
Chytridiomycota
Others(<0.5%)
Glomeromycota
Mucoromycota
Entorrhizomycota
Aphelidiomycota
Unclassified
Proteobacteria
Bacteroidetes
Acidobacteria
Actinobacteria
Verrucomicrobia
Chloroflexi
TM7
Planctomycetes
Gemmatimonadetes
Firmicutes
Others(<0.5%)
OD1
Chlamydiae
Cyanobacteria
Elusimicrobia
Nitrospirae
TM6
Chlorobi
WS3

Fi g. 4

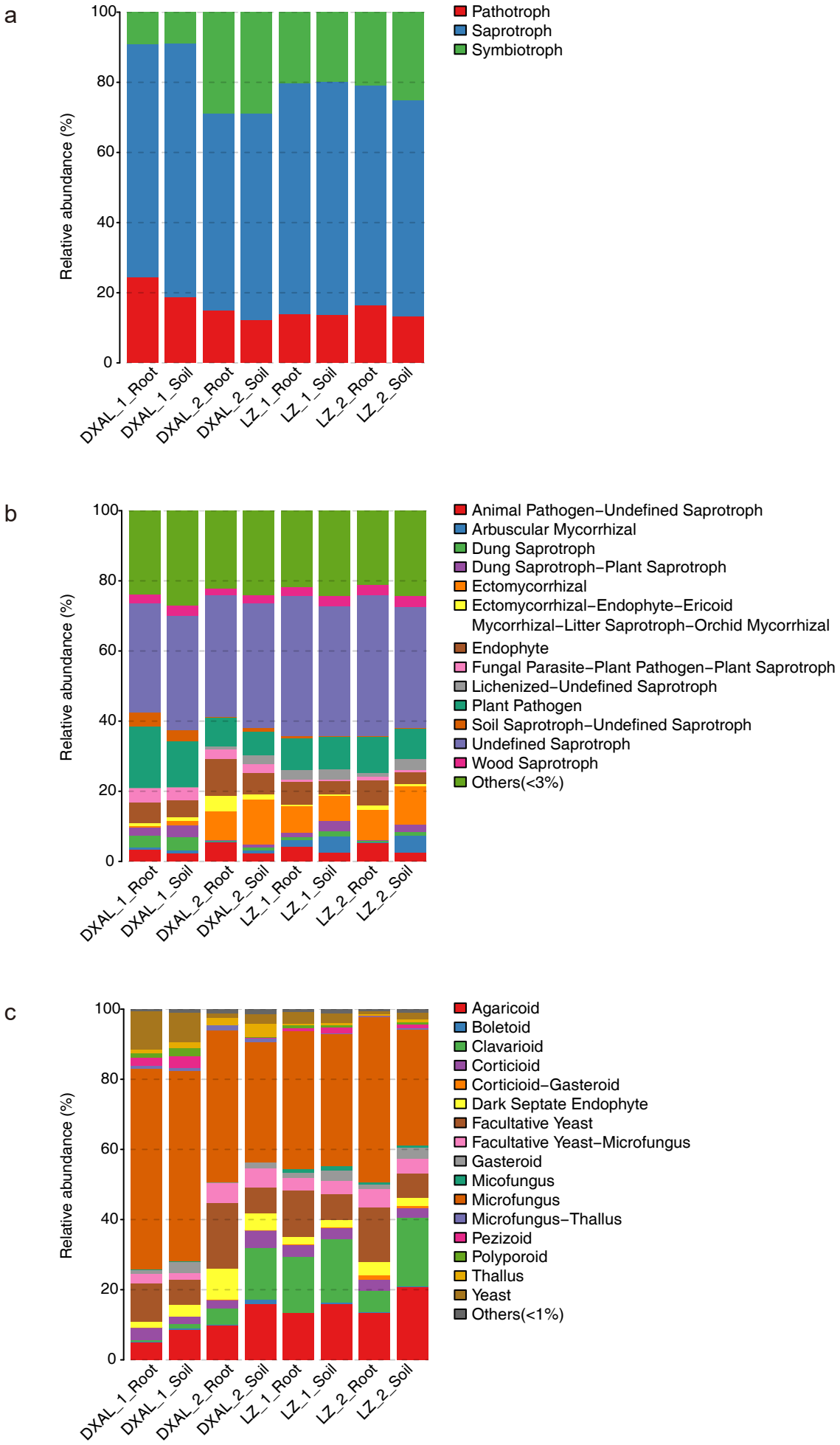
a
Relative abundance (%)
100
80
60
40
20
0
DXAL_1_Root
DXAL_1_Soil
DXAL_2_Root
DXAL_2_Soil
LZ_1_Root
LZ_1_Soil
LZ_2_Root
LZ_2_Soil
Pathotroph
Saprotroph
Symbiotroph
b
Relative abundance (%)
Animal Pathogen−Undefined Saprotroph
Arbuscular Mycorrhizal
Dung Saprotroph
Dung Saprotroph−Plant Saprotroph
Ectomycorrhizal
Ectomycorrhizal−Endophyte−Ericoid Mycorrhizal−Litter Saprotroph−Orchid Mycorrhizal
Endophyte
Fungal Parasite−Plant Pathogen−Plant Saprotroph
Lichenized−Undefined Saprotroph
Plant Pathogen
Soil Saprotroph−Undefined Saprotroph
Undefined Saprotroph
Wood Saprotroph
Others(<3%)
c
Relative abundance (%)
Agaricoid
Boletoid
Clavarioid
Corticioid
Corticioid−Gasteroid
Dark Septate Endophyte
Facultative Yeast
Facultative Yeast−Microfungus
Gasteroid
Micofungus
Microfungus
Microfungus−Thallus
Pezizoid
Polyporoid
Thallus
Yeast
Others(<1%)


Fi g. 5
DXAL_1
DXAL_2
LZ_1
LZ_2
M00360:Aminoacyl−tRNA biosynthesis, prokaryotes
M00359:Aminoacyl−tRNA biosynthesis, eukaryotes
M00023:Tryptophan biosynthesis, chorismate => tryptophan
M00551:Benzoate degradation, benzoate => catechol / methylbenzoate => methylcatechol
M00543:Biphenyl degradation, biphenyl => 2−oxopent−4−enoate + benzoate
M00419:Cymene degradation, p−cymene => p−cumate
M00417:Cytochrome o ubiquinol oxidase
M00159:V−type ATPase, prokaryotes
M00145:NAD(P)H:quinone oxidoreductase, chloroplasts and cyanobacteria
M00144:NADH:quinone oxidoreductase, prokaryotes
M00429:Competence−related DNA transformation transporter
M00335:Sec (secretion) system
M00334:Type VI secretion system
M00333:Type IV secretion system
M00332:Type III secretion system
M00036:Leucine degradation, leucine => acetoacetate + acetyl−CoA
M00019:Valine/isoleucine biosynthesis, pyruvate => valine / 2−oxobutanoate => isoleucine
M00620:Incomplete reductive citrate cycle, acetyl−CoA => oxoglutarate
M00377:Reductive acetyl−CoA pathway (Wood−Ljungdahl pathway)
M00375:Hydroxypropionate−hydroxybutylate cycle
M00374:Dicarboxylate−hydroxybutyrate cycle
M00173:Reductive citrate cycle (Arnon−Buchanan cycle)
M00307:Pyruvate oxidation, pyruvate => acetyl−CoA
M00008:Entner−Doudoroff pathway, glucose−6P => glyceraldehyde−3P + pyruvate
M00125:Riboflavin biosynthesis, GTP => riboflavin/FMN/FAD
M00122:Cobalamin biosynthesis, cobinamide => cobalamin
M00120:Coenzyme A biosynthesis, pantothenate => CoA
M00116:Menaquinone biosynthesis, chorismate => menaquinone
M00709:Macrolide resistance, MacAB−TolC transporter
M00721:Cationic antimicrobial peptide (CAMP) resistance, arnBCADTEF operon
M00319:Manganese/zinc/iron transport system
M00317:Manganese/iron transport system
M00247:Putative ABC transport system
M00245:Cobalt/nickel transport system
M00378:F420 biosynthesis
M00302:2−Aminoethylphosphonate transport system
M00301:Mannopine transport system
M00300:Putrescine transport system
M00208:Glycine betaine/proline transport system
M00193:Putative spermidine/putrescine transport system
M00191:Thiamine transport system
M00362:Nucleotide sugar biosynthesis, prokaryotes
M00542:EHEC/EPEC pathogenicity signature, T3SS and effectors
M00349:Microcin C transport system
M00348:Glutathione transport system
M00324:Dipeptide transport system
M00239:Peptides/nickel transport system
M00238:D−Methionine transport system
M00236:Putative polar amino acid transport system
M00235:Arginine/ornithine transport system
M00232:General L−amino acid transport system
M00231:Octopine/nopaline transport system
M00228:Putative glutamine transport system
M00226:Histidine transport system
M00225:Lysine/arginine/ornithine transport system
M00660:Xanthomonas spp. pathogenicity signature, T3SS and effectors
M00342:Bacterial proteasome
M00546:Purine degradation, xanthine => urea
M00049:Adenine ribonucleotide biosynthesis, IMP => ADP,ATP
M00048:Inosine monophosphate biosynthesis, PRPP + glutamine => IMP
M00051:Uridine monophosphate biosynthesis, glutamine (+ PRPP) => UMP
M00046:Pyrimidine degradation, uracil => beta−alanine, thymine => 3−aminoisobutanoate
M00179:Ribosome, archaea
M00178:Ribosome, bacteria
M00183:RNA polymerase, bacteria
M00221:Putative simple sugar transport system
M00220:Rhamnose transport system
M00218:Fructose transport system
M00216:Multiple sugar transport system
M00213:L−Arabinose transport system
M00207:Putative multiple sugar transport system
M00204:Trehalose/maltose transport system
M00202:Oligogalacturonide transport system
M00201:alpha−Glucoside transport system
M00200:Putative sorbitol/mannitol transport system
M00199:L−Arabinose/lactose transport system
M00198:Putative sn−glycerol−phosphate transport system
M00196:Multiple sugar transport system
M00664:Nodulation
M00504:DctB−DctD (C4−dicarboxylate transport) two−component regulatory system
M00485:KinABCDE−Spo0FA (sporulation control) two−component regulatory system
Aminoacyl tRNA
Aromatic amino acid metabolism
Aromatics degradation
ATP synthesis
Bacterial secretion system
Branched−chain amino acid metabolism
Carbon fixation
Central carbohydrate metabolism
Cofactor and vitamin biosynthesis
Drug efflux transporter/pump
Drug resistance
Metallic cation, iron−siderophore and vitamin B12 transport system
Methane metabolism
Mineral and organic ion transport system
Nucleotide sugar
Pathogenicity
Peptide and nickel transport system
Phosphate and amino acid transport system
Plant pathogenicity
Proteasome
Purine metabolism
Pyrimidine metabolism
Ribosome
RNA polymerase
Saccharide, polyol, and lipid transport system
Symbiosis
Two−component regulatory system
−3 0 3 6
−4 0 4 8
−5 0 5
−2.5 0.0 2.5 5.0
Z−score

Fi g. 6

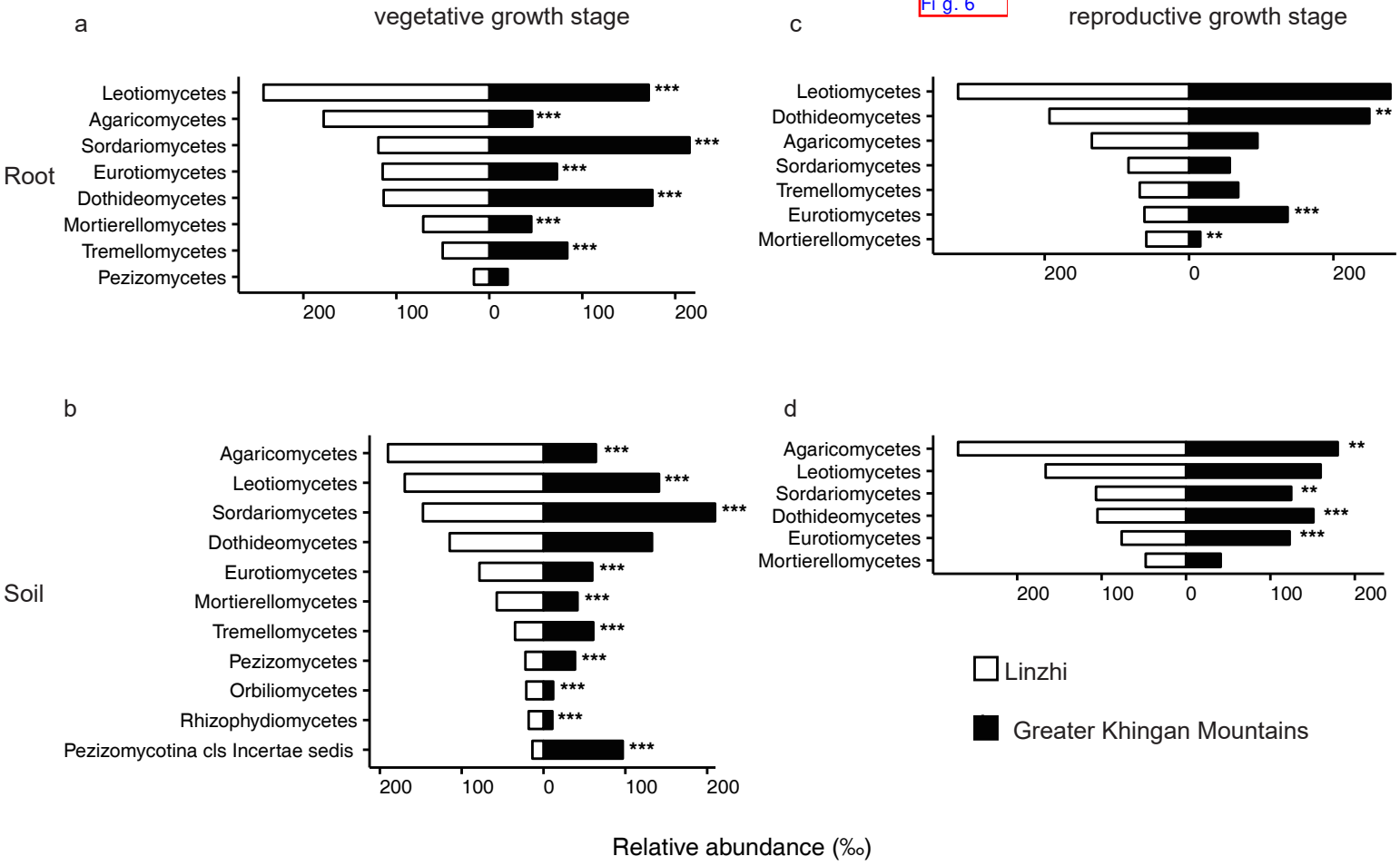
a
vegetative growth stage
c
reproductive growth stage
Root
Leotiomycetes
Agaricomycetes
Sordariomycetes
Eurotiomycetes
Dothideomycetes
Mortierellomycetes
Tremellomycetes
Pezizomycetes
Dothideomycetes
Tremellomycetes
***
**
200
100
0
b
d
Soil
Agaricomycetes
Leotiomycetes
Sordariomycetes
Dothideomycetes
Eurotiomycetes
Mortierellomycetes
Tremellomycetes
Pezizomycetes
Orbiliomycetes
Rhizophydiomycetes
Pezizomycotina cls Incertae sedis
Linzhi
Greater Khingan Mountains
Relative abundance (‰)

Root Fi g. 7

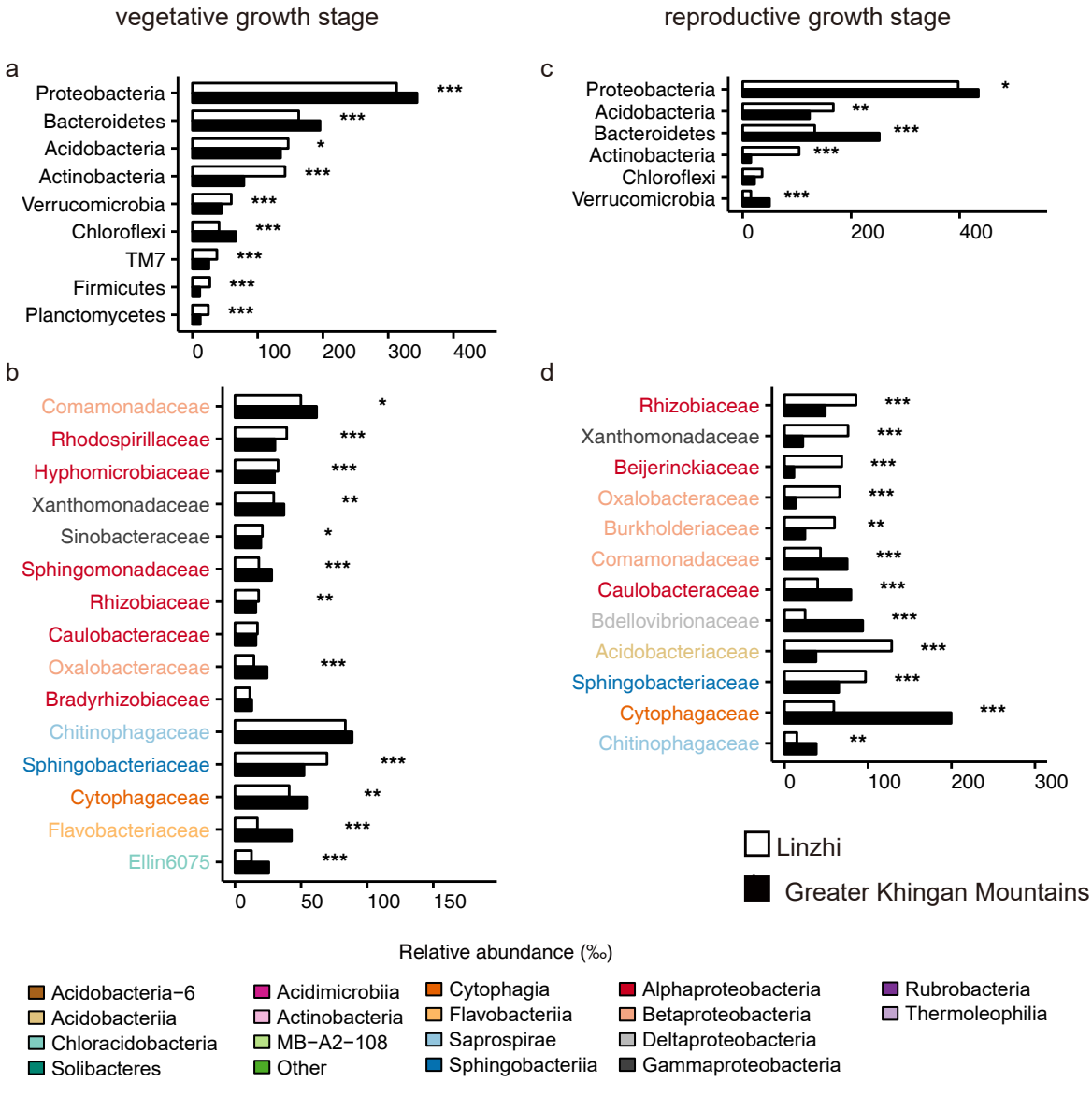
vegetative growth stage
reproductive growth stage
a
Proteobacteria
Bacteroidetes
Acidobacteria
Actinobacteria
Verrucomicrobia
Chloroflexi
TM7
Firmicutes
Planctomycetes
0
100
200
300
400
c
Proteobacteria
Acidobacteria
Bacteroidetes
Actinobacteria
Chloroflexi
Verrucomicrobia
0
200
400
b
Comamonadaceae
Rhodospirillaceae
Hyphomicrobiaceae
Xanthomonadaceae
Sinobacteraceae
Sphingomonadaceae
Rhizobiaceae
Caulobacteraceae
Oxalobacteraceae
Bradyrhizobiaceae
Chitinophagaceae
Sphingobacteriaceae
Cytophagaceae
Flavobacteriaceae
Ellin6075
0
50
100
150
d
Rhizobiaceae
Xanthomonadaceae
Beijerinckiaceae
Oxalobacteraceae
Burkholderiaceae
Comamonadaceae
Caulobacteraceae
Bdellovibrionaceae
Acidobacteriaceae
Sphingobacteriaceae
Cytophagaceae
Chitinophagaceae
0
100
200
300
Linzhi
Greater Khingan Mountains
Relative abundance (‰)
Acidobacteria−6
Acidobacteriia
Chloracidobacteria
Solibacteres
Acidimicrobiia
Actinobacteria
MB−A2−108
Other
Cytophagia
Flavobacteriia
Saprospirae
Sphingobacteriia
Alphaproteobacteria
Betaproteobacteria
Deltaproteobacteria
Gammaproteobacteria
Rubrobacteria
Thermoleophilia

Fi g. 8

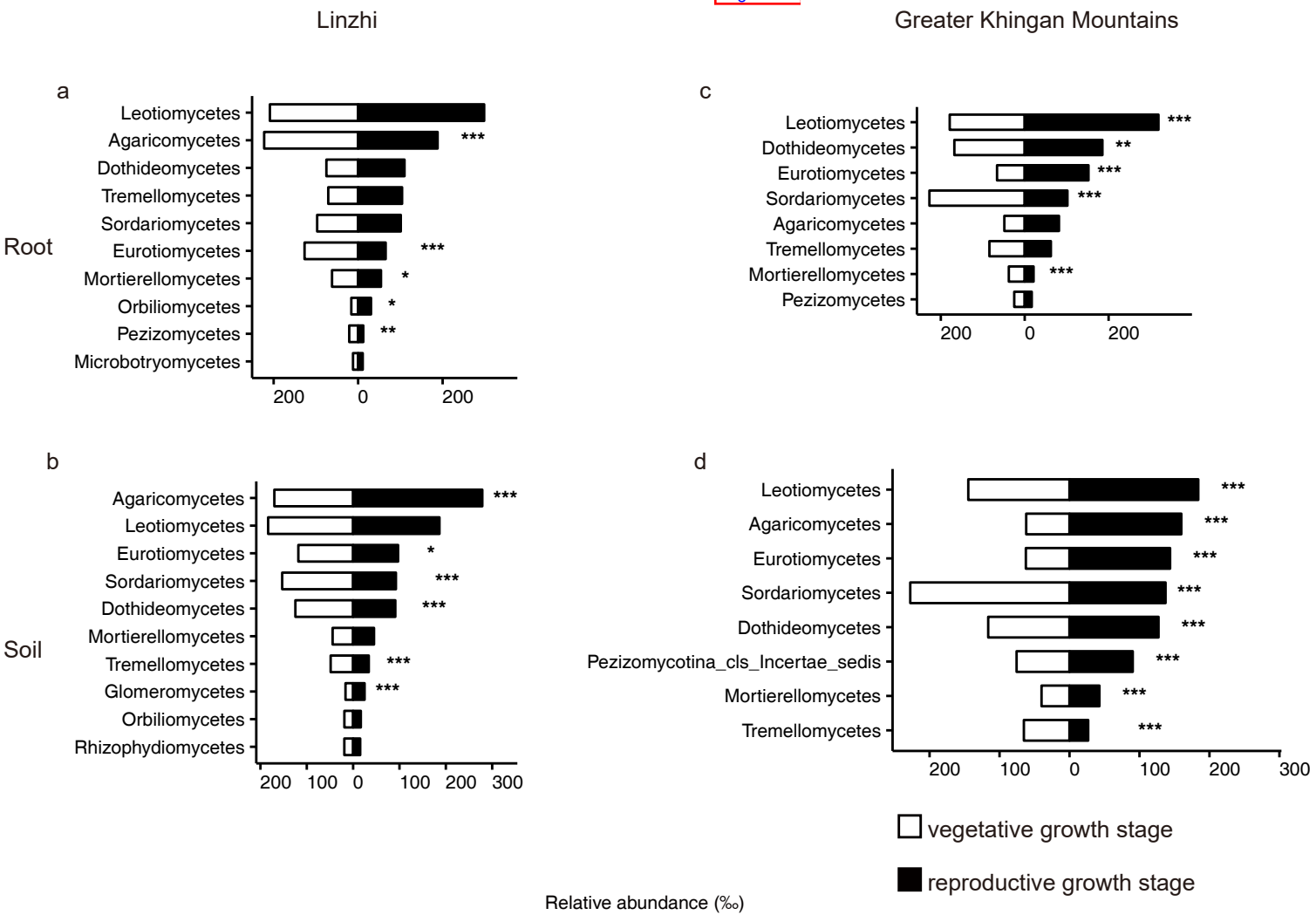
Linzhi
Greater Khingan Mountains
a
Root
Leotiomycetes
Agaricomycetes
Dothideomycetes
Tremellomycetes
Sordariomycetes
Eurotiomycetes
Mortierellomycetes
Orbiliomycetes
Pezizomycetes
Microbotryomycetes
***
***
*
*
**
200
0
200
c
Leotiomycetes
Dothideomycetes
Eurotiomycetes
Sordariomycetes
Agaricomycetes
Tremellomycetes
Mortierellomycetes
Pezizomycetes
***
**
***
***
***
200
0
200
b
Soil
Agaricomycetes
Leotiomycetes
Eurotiomycetes
Sordariomycetes
Dothideomycetes
Mortierellomycetes
Tremellomycetes
Glomeromycetes
Orbiliomycetes
Rhizophydiomycetes
***
***
*
***
***
***
***
200
100
0
100
200
300
d
Leotiomycetes
Agaricomycetes
Eurotiomycetes
Sordariomycetes
Dothideomycetes
Pezizomycotina_cls_Incertae_sedis
Mortierellomycetes
Tremellomycetes
***
***
***
***
***
***
***
***
200
100
0
100
200
300
vegetative growth stage
reproductive growth stage
Relative abundance (‰)

Root

Fi g. 9

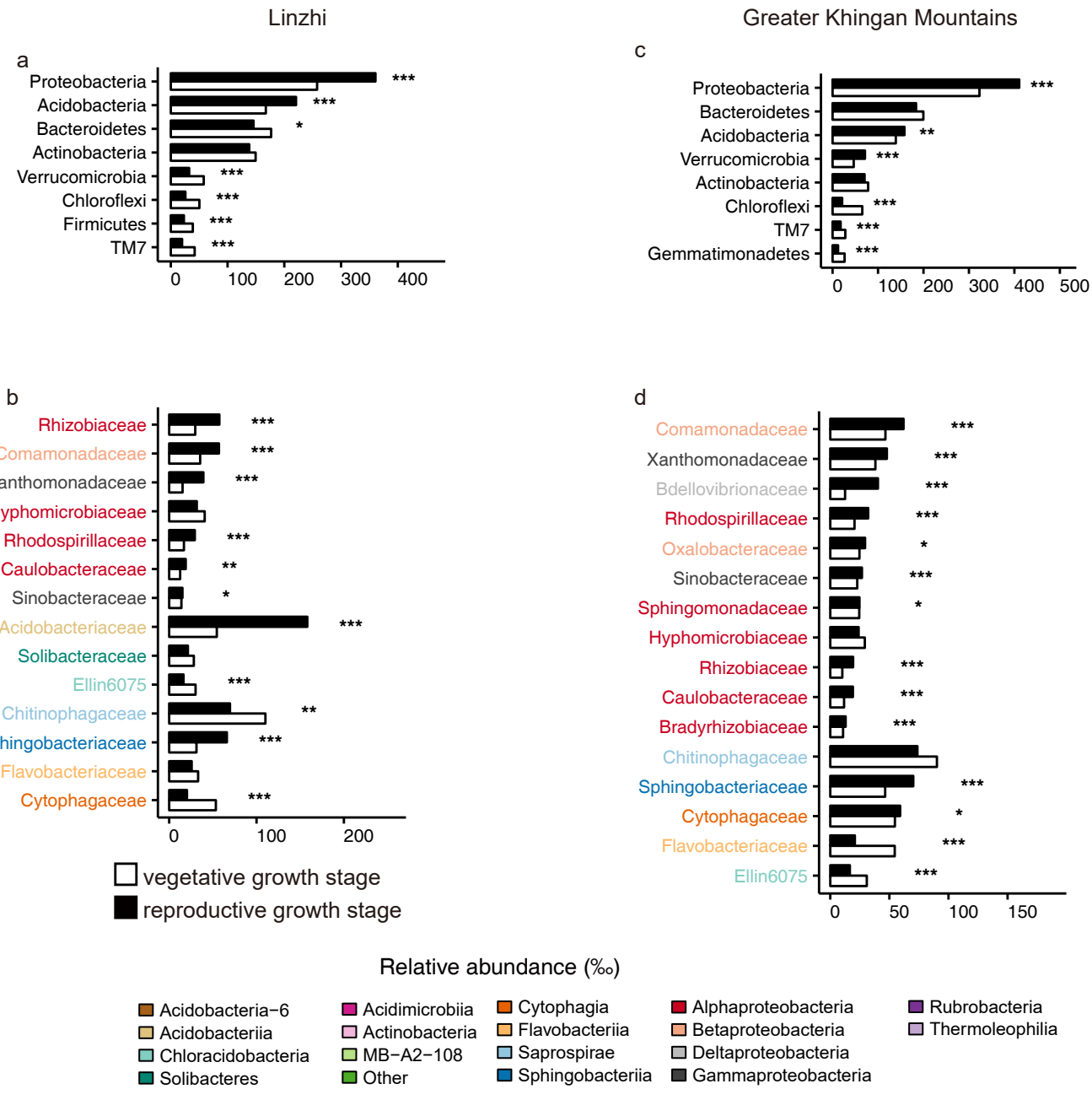
Linzhi
Greater Khingan Mountains
a
Proteobacteria
Acidobacteria
Bacteroidetes
Actinobacteria
Verrucomicrobia
Chloroflexi
Firmicutes
TM7
0
100
200
300
400
c
Proteobacteria
Bacteroidetes
Acidobacteria
Verrucomicrobia
Actinobacteria
Chloroflexi
TM7
Gemmatimonadetes
0
100
200
300
400
500
b
Rhizobiaceae
Comamonadaceae
Xanthomonadaceae
Hyphomicrobiaceae
Rhodospirillaceae
Caulobacteraceae
Sinobacteraceae
Acidobacteriaceae
Solibacteraceae
Ellin6075
Chitinophagaceae
Sphingobacteriaceae
Flavobacteriaceae
Cytophagaceae
0
100
200
vegetative growth stage
reproductive growth stage
d
Comamonadaceae
Xanthomonadaceae
Bdellovibrionaceae
Rhodospirillaceae
Oxalobacteraceae
Sinobacteraceae
Sphingomonadaceae
Hyphomicrobiaceae
Rhizobiaceae
Caulobacteraceae
Bradyrhizobiaceae
Chitinophagaceae
Sphingobacteriaceae
Cytophagaceae
Flavobacteriaceae
Ellin6075
0
50
100
150
Relative abundance (‰)
Acidobacteria−6
Acidobacteriia
Chloracidobacteria
Solibacteres
Acidimicrobiia
Actinobacteria
MB−A2−108
Other
Cytophagia
Flavobacteriia
Saprospirae
Sphingobacteriia
Alphaproteobacteria
Betaproteobacteria
Deltaproteobacteria
Gammaproteobacteria
Rubrobacteria
Thermoleophilia

Figures

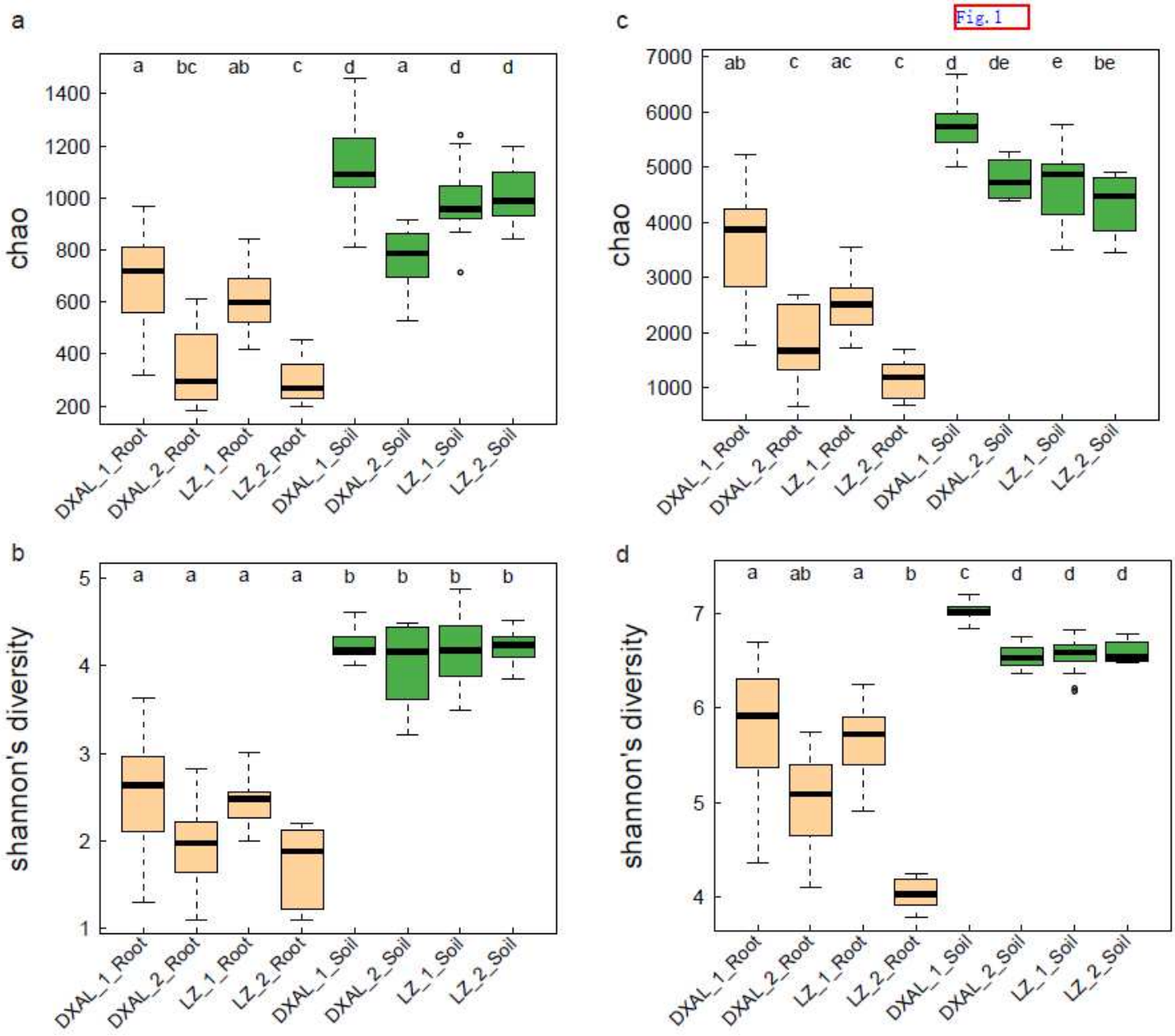

Figure 1

Species richness and diversity of root-associated microbial communities. a Microbial richness index comparison between each group based on the Chao index using the ITS data. b Microbial diversity index comparison between each group based on the Shannon index using the ITS data. c Microbial richness index comparison between each group based on the Chao index using the 16S rRNA gene data. d Microbial diversity index comparison between each group based on the Shannon index using the 16S rRNA gene data. Significant differences are depicted with letters ($p < 0.05$, Kruskal-Wallis with Dunn's post hoc test). DXAL: Greater Khingan Mountains, LZ: Linzhi, 1: vegetative growth stage, 2: reproductive growth stage

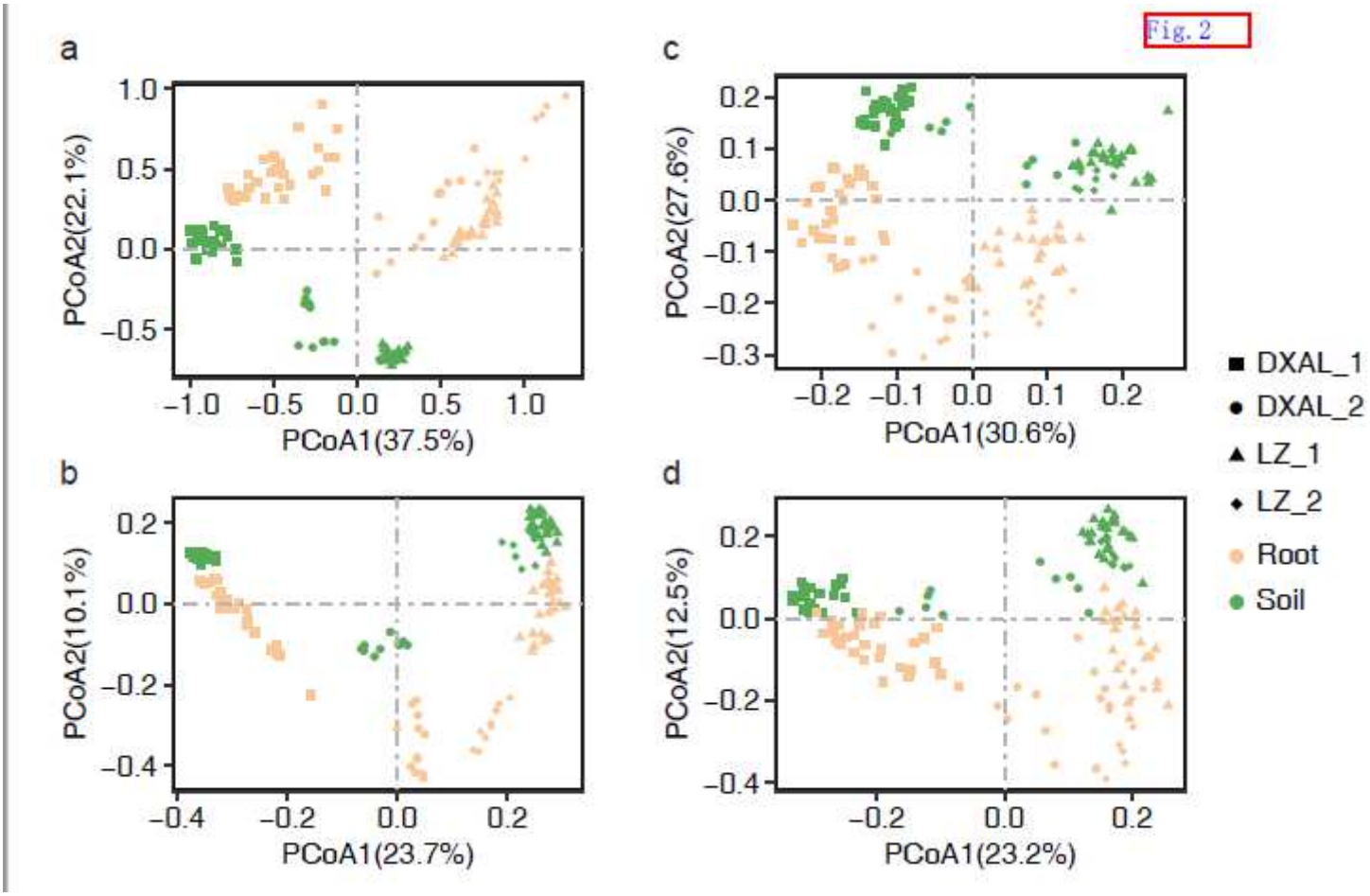

Figure 4

Principal coordinate analyses (PCoAs) of microbial community composition among different sample types of G. conopsea. a PCoA using the weighted UniFrac (WUF) distances at the OTU level using fungal community's data. b PCoA using the unweighted UniFrac (UUF) distances at the OTU level using fungal community's data. c PCoA using the weighted UniFrac (WUF) distances at the OTU level using bacterial community's data. d PCoA using the unweighted UniFrac (UUF) distances at the OTU level using bacterial community's data. Samples are color coded according to the sites, compartments, and developmental stages are depicted with different symbols. DXAL: Greater Khingan Mountains, LZ: Linzhi, 1: vegetative growth stage, 2: reproductive growth stage

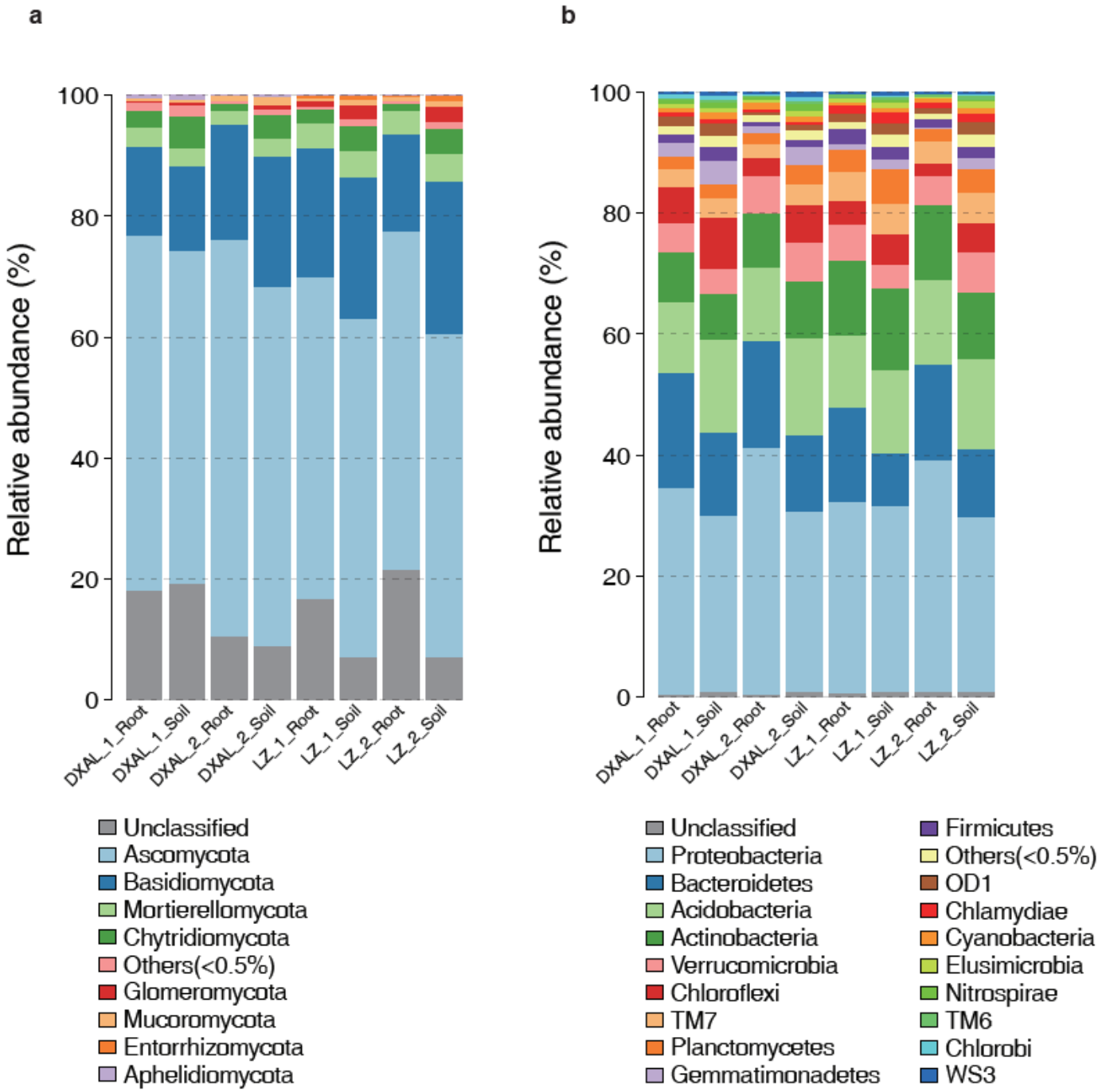

Figure 6

Microbial community composition among different sample types of G. conopsea at phylum level. a Relative abundance of fungal taxa of each group. b Relative abundance of bacterial taxa of each group. DXAL: Greater Khingan Mountains, LZ: Linzhi, 1: vegetative growth stage, 2: reproductive growth stage

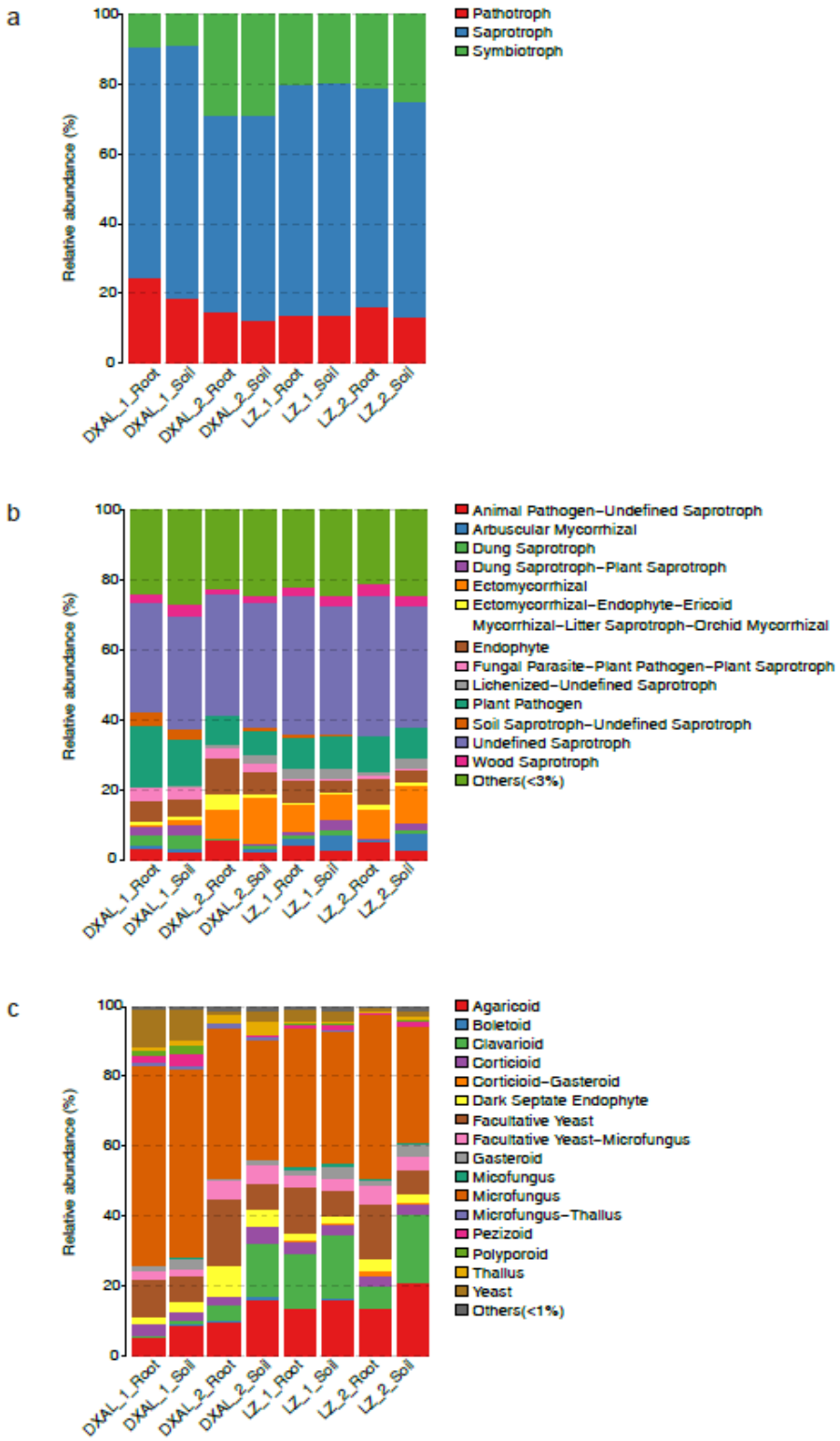

Figure 8

Compositions of fungal functional group (guild) inferred by FUNGuild. a At the trophic mode level. b At guilds level. c At Growth_Morphology level. DXAL: Greater Khingan Mountains, LZ: Linzhi, 1: vegetative growth stage, 2: reproductive growth stage

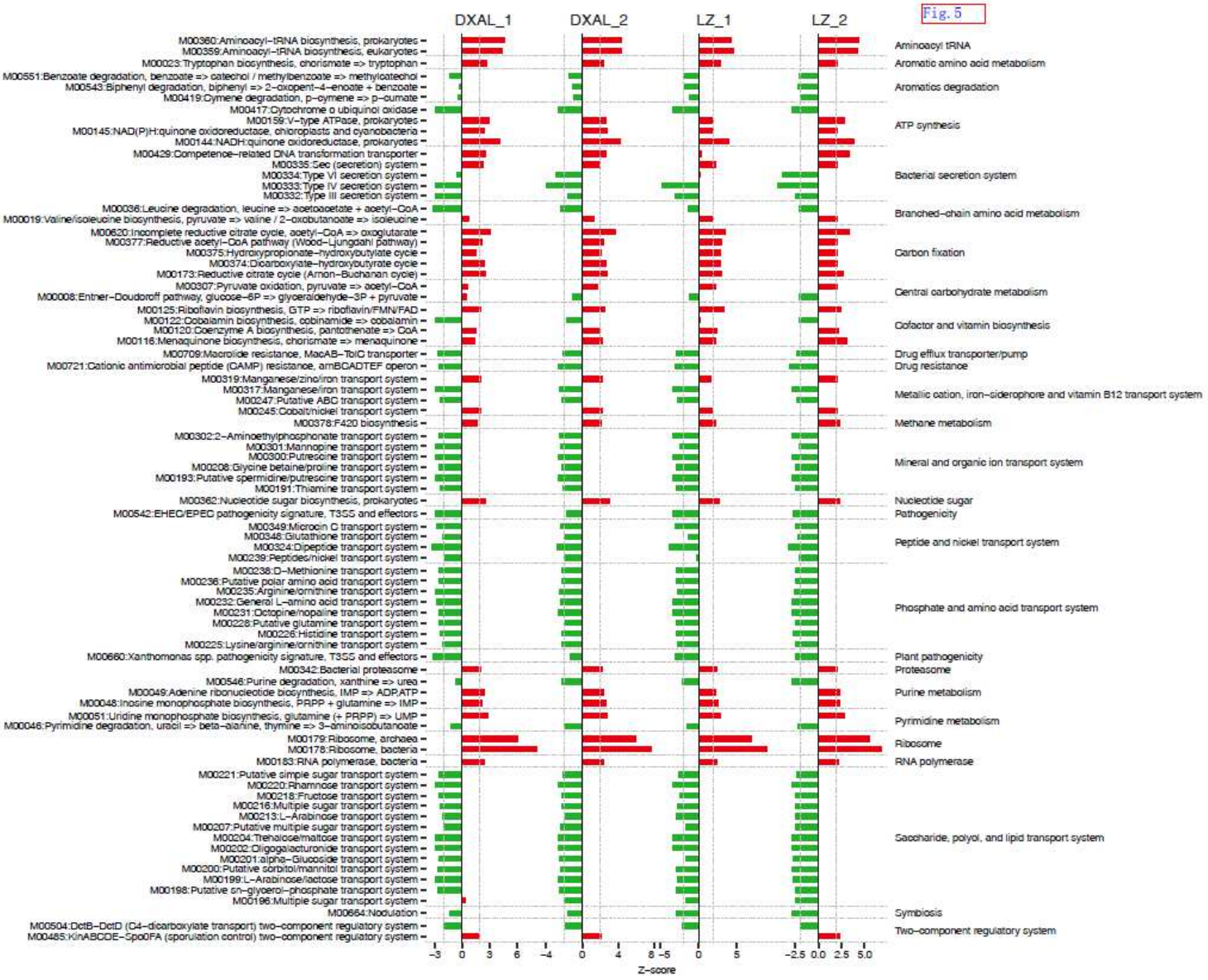

Figure 10

Alterations in bacteria microbial functional modules in each compare group. Dashed lines indicate a reporter score of 1.96, corresponding to 95% confidence in a normal distribution. DXAL_1: DXAL_1_Root vs DXAL_1_Soil, DXAL_2: DXAL_2_Root vs DXAL_2_Soil, LZ_1: LZ_1_Root vs LZ_1_Soil, LZ_2: LZ_2_Root vs LZ_2_Soil. DXAL: Greater Khingan Mountains, LZ: Linzhi, 1: vegetative growth stage, 2: reproductive growth stage

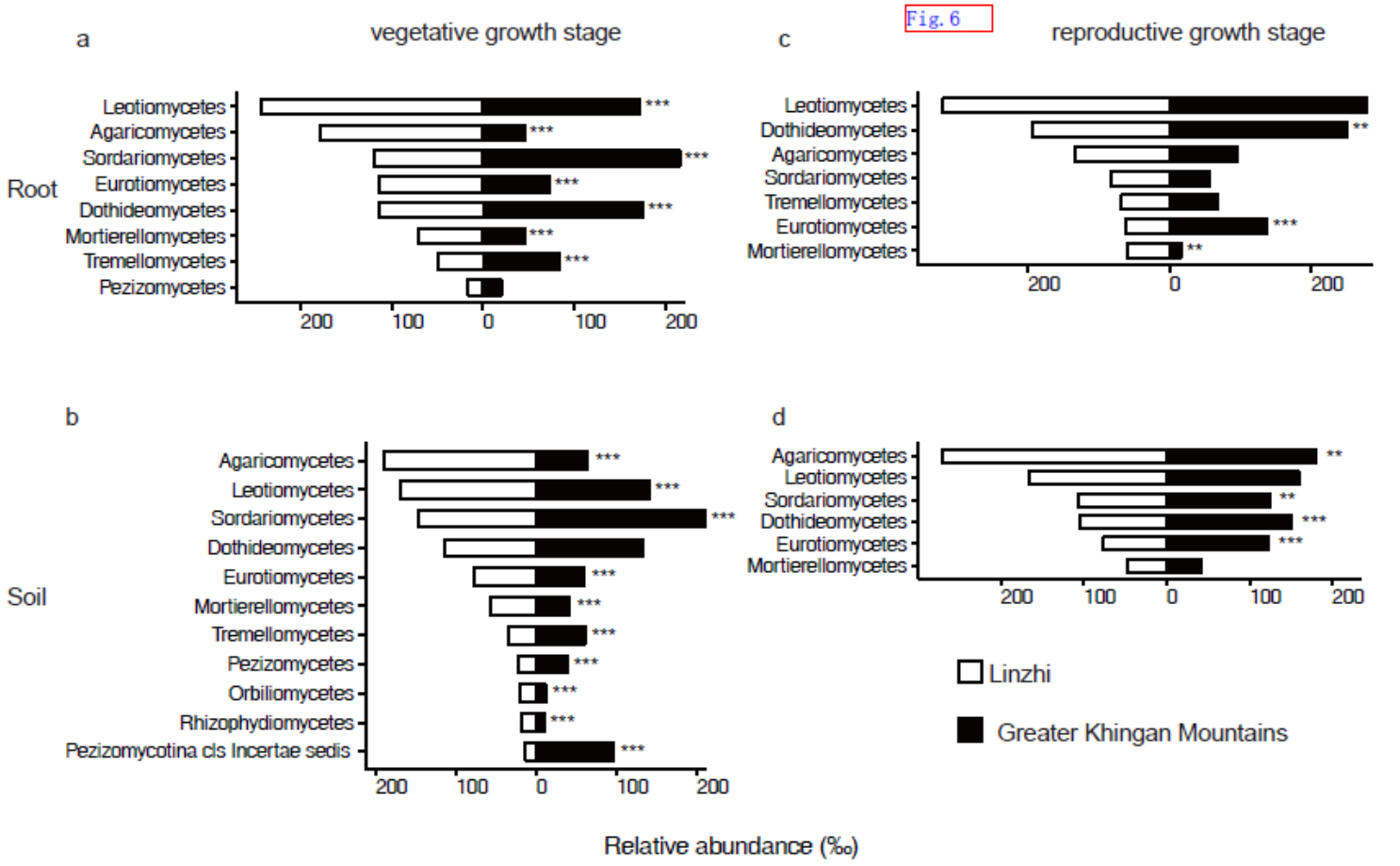

Figure 12

Side-by-side comparison of the relative abundance (‰) of classes which made up at least >10‰ of the total fungal core microbiome community across different sites. a Relative abundance (‰) of the classes detected in root core OTUs of the indicated plant growth sites at vegetative growth stage. b Relative abundance (‰) of the classes detected in soil core OTUs of the indicated plant growth sites at vegetative growth stage. c Relative abundance (‰) of the classes detected in root core OTUs of the indicated plant growth sites at reproductive growth stage. d Relative abundance (‰) of the classes detected in soil core OTUs of the indicated plant growth sites at reproductive growth stage. Asterisks indicate significant differences occur between Linzhi and Greater Khingan Mountains (Benjamini–Hochberg false discovery-rate (FDR) adjusted P value, * represent < 0.05, ** represent < 0.01, *** represent < 0.001) in each compartment.

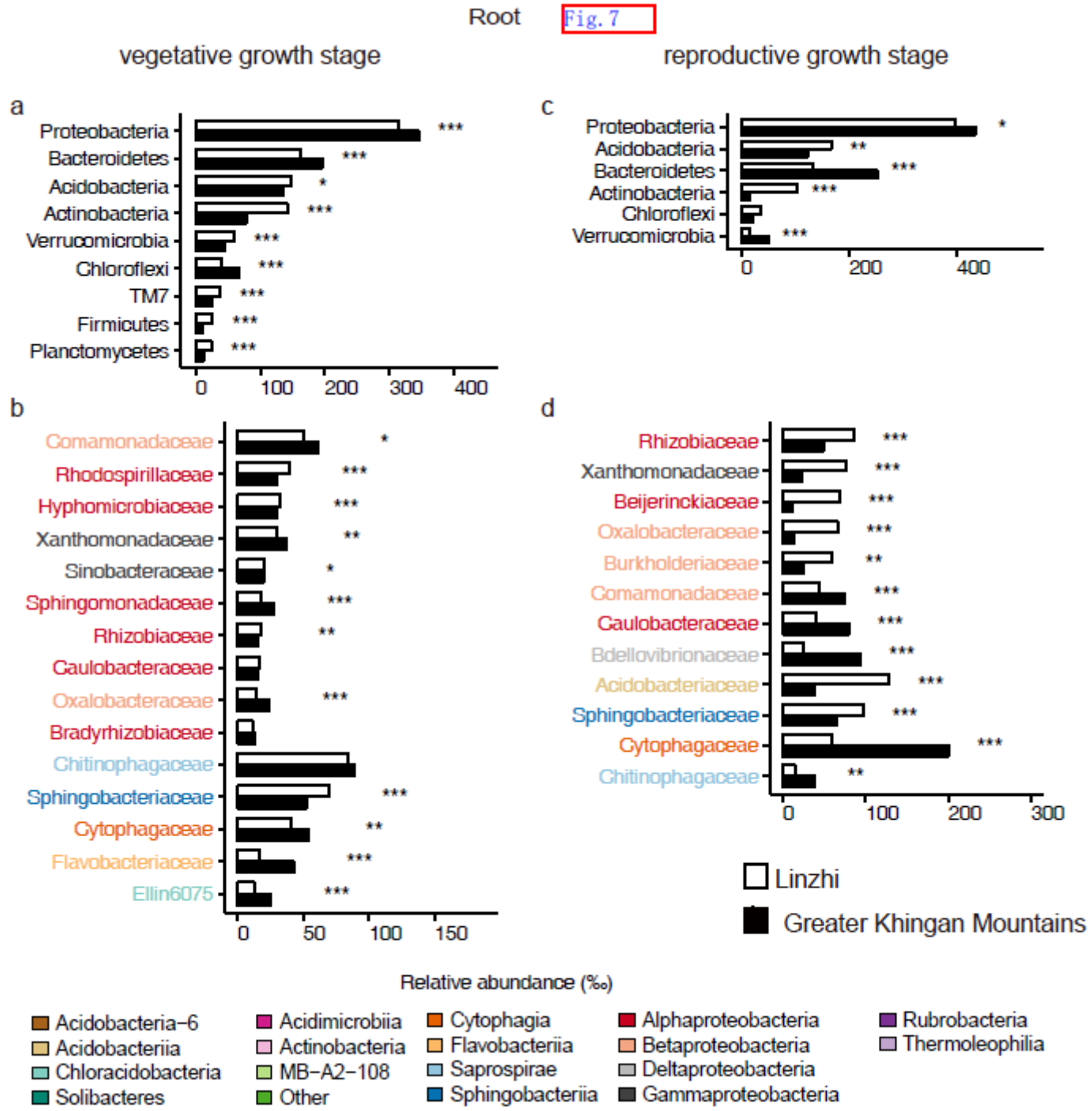

Figure 14

Comparative analyses of bacterial core microbiome across different sites. a Relative abundance (‰) of the phyla detected in root core OTUs of the indicated plant growth sites at vegetative growth stage. b Relative abundance (‰ of families belonging to the three dominant phyla in the root core OTUs of the indicated plant growth sites at vegetative growth stage. c Relative abundance (‰) of the phyla detected in root core OTUs of the indicated plant growth sites at reproductive growth stage. d Relative abundance (‰ of families belonging to the three dominant phyla in the root core OTUs of the indicated plant growth sites at reproductive growth stage. Asterisks indicate significant differences (Benjamini–Hochberg false discovery-rate (FDR) adjusted P value, * represent < 0.05, ** represent < 0.01, *** represent < 0.001).

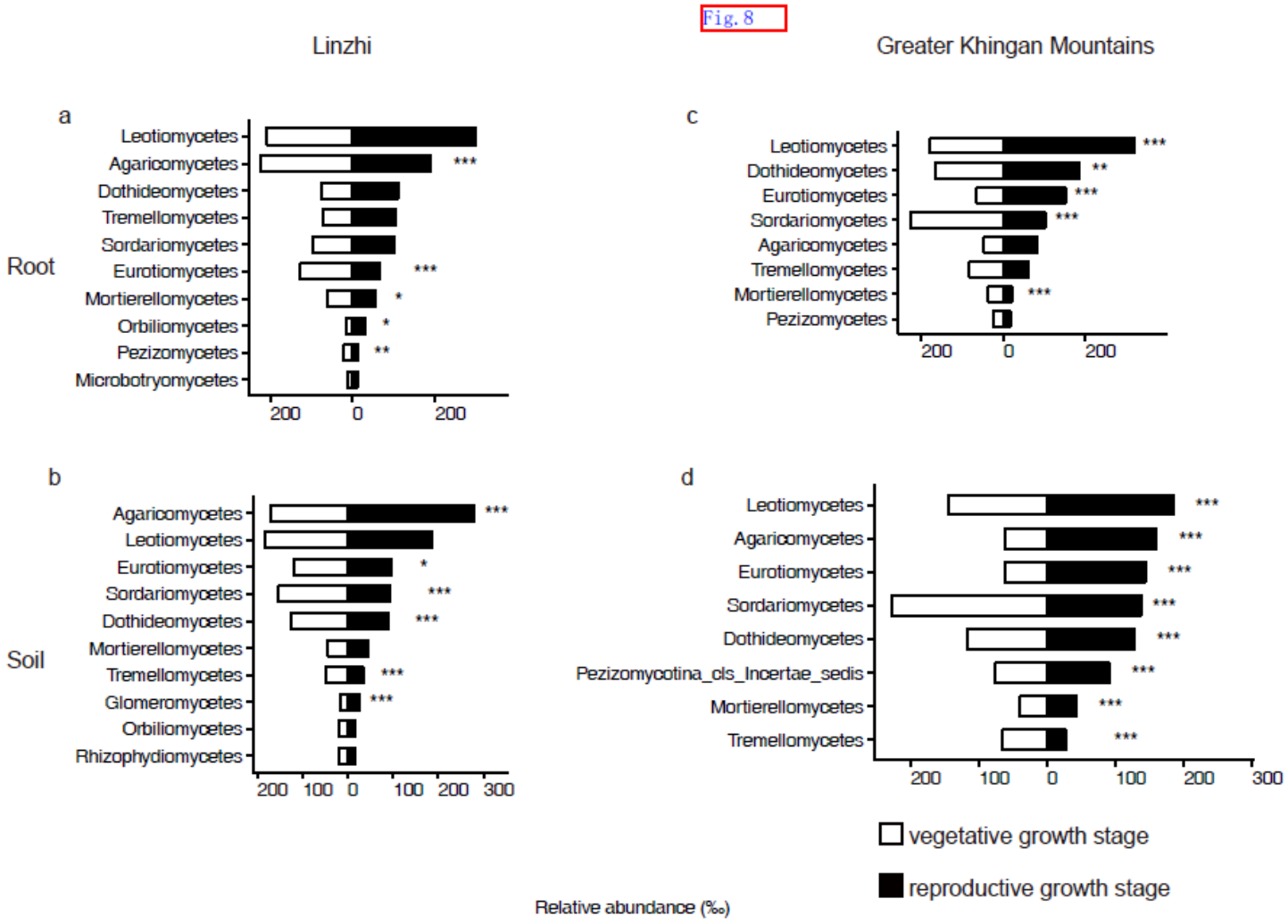

Figure 16

Side-by-side comparison of the relative abundance (‰) of classes which made up at least >10‰ of the total fungal core microbiome community across different developmental stages. a Relative abundance (‰) of the classes detected in root core OTUs of the indicated developmental stages in Linzhi. b Relative abundance (‰) of the classes detected in soil core OTUs of the indicated plant growth sites in Linzhi. c Relative abundance (‰) of the classes detected in root core OTUs of the indicated plant growth sites in Greater Khingan Mountains. d Relative abundance (‰) of the classes detected in soil core OTUs of the indicated plant growth sites in Greater Khingan Mountains. Asterisks indicate significant differences occur between vegetative growth stage and reproductive growth stage (Benjamini–Hochberg false discovery-rate (FDR) adjusted P value, * represent < 0.05, ** represent < 0.01, *** represent < 0.001) in each compartment.

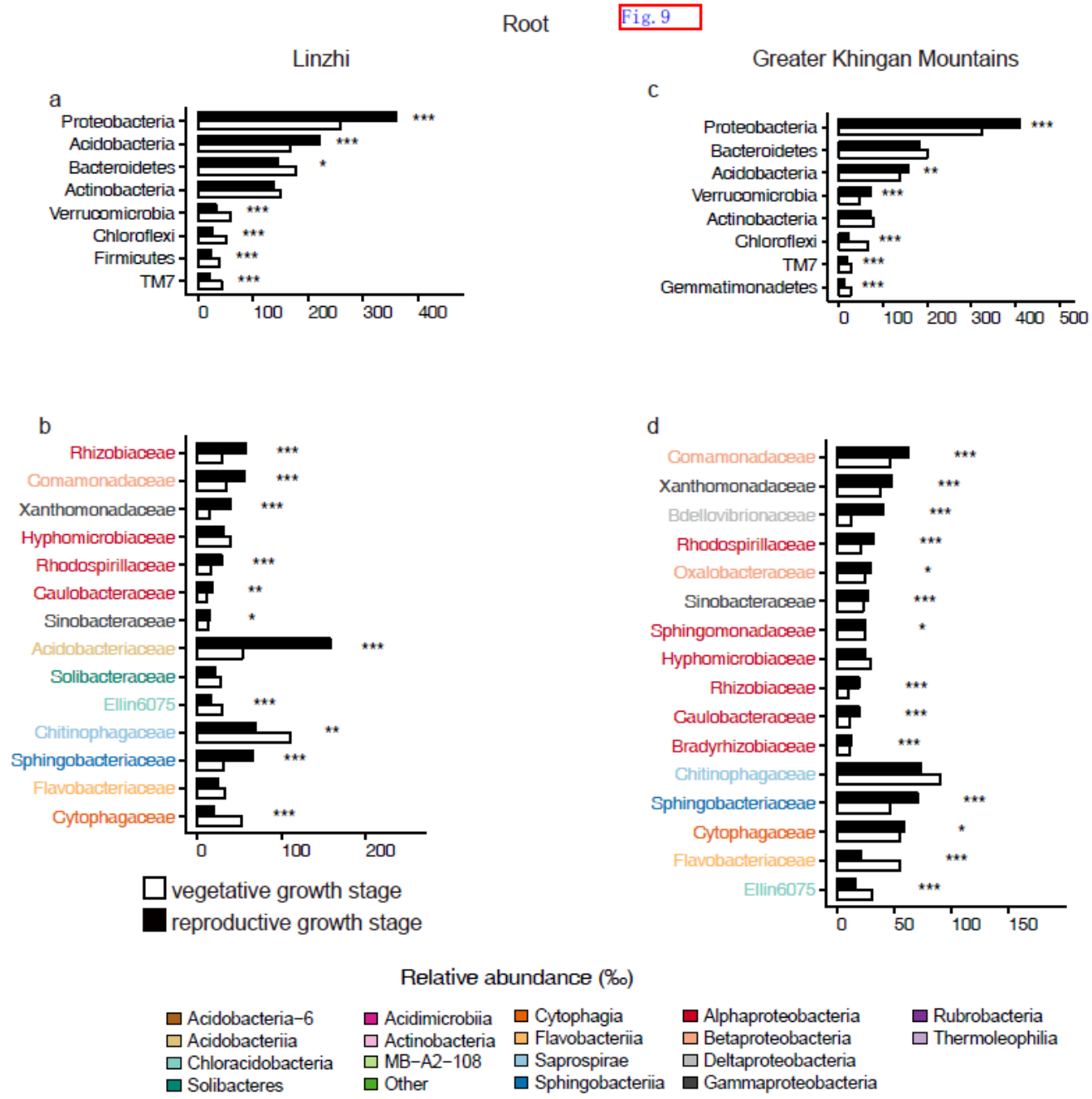

Figure 18

Comparative analyses of bacterial core microbiome across different developmental stages. a Relative abundance (‰) of the phyla detected in root core OTUs of the indicated developmental stages in Linzhi. b Relative abundance (‰ of families belonging to the three dominant phyla in the root core OTUs of the indicated developmental stages in Linzhi. c Relative abundance (‰) of the phyla detected in root core OTUs of the indicated plant growth sites in Greater Khingan Mountains. d Relative abundance (‰ of families belonging to the three dominant phyla in the root core OTUs of the indicated plant growth sites in Greater Khingan Mountains. Asterisks indicate significant differences (Benjamini–Hochberg false discovery-rate (FDR) adjusted P value, * represent < 0.05, ** represent < 0.01, *** represent < 0.001).

Supplementary Files

This is a list of supplementary files associated with this preprint. Click to download.

- TableS10.xlsx
- TableS2.xlsx
- TableS14.xlsx
- TableS13.xlsx
- TableS12.xlsx
- TableS7.xlsx
- TableS11.xlsx
- TableS10.xlsx
- TableS9.xlsx
- TableS8.xlsx
- TableS7.xlsx
- TableS1.xlsx
- TableS1.xlsx
- TableS11.xlsx
- TableS6.xlsx
- TableS12.xlsx
- TableS13.xlsx
- TableS14.xlsx
- TableS3.xlsx
- AdditionalfilesFigureS.pdf
- TableS4.xlsx
- AdditionalfilesFigureS.pdf
- TableS3.xlsx
- TableS9.xlsx
- TableS4.xlsx
- TableS6.xlsx
- TableS5.xlsx
- TableS8.xlsx
- TableS2.xlsx
- TableS5.xlsx